AFRL-VS-HA-TR-98-0039

# Systematic Differences in the Spectral Excitation of Pn and Lg by the Last Lop Nor Explosions and Nearby Earthquakes: Implications on the Pn/Lg Spectral Ratio Discriminant

Jiakang Xie

St. Louis University
Department of Earth and Atmospheric Sciences
3507 Laclede Ave.
St. Louis, MO 63103

1 February 1998

Final Report
1 October 1996 - 30 November 1997

**DEPARTMENT OF ENERGY
OFFICE OF NON-PROLIFERATION AND
 NATIONAL SECURITY
WASHINGTON, DC 20585**

**AIR FORCE RESEARCH LABORATORY
Space Vehicles Directorate
29 Randolph Road
AIR FORCE MATERIEL COMMAND
HANSCOM AFB, MA 01731-3010**

19980915 062

# REPORT DOCUMENTATION PAGE

| 1. AGENCY USE ONLY *(Leave blank)* | 2. REPORT DATE <br> 1 February 1998 | 3. REPORT TYPE AND DATES COVERED <br> Final (1 Oct. 1996 – 30 Nov. 1997) |
|---|---|---|

| 4. TITLE AND SUBTITLE <br> Systematic Differences in the Spectral Excitation of Pn and Lg by the Last Lop Nor Explosions and Nearby Earthquakes: Implication for the Pn/Lg Spectral Ratio Discriminant | 5. FUNDING NUMBERS <br> F19628-95-K-0013 <br> PE 69120H <br> PR DENN <br> TA GM <br> WU AR |
|---|---|
| 6. AUTHOR(S) <br><br> Jiakang Xie* | |

| 7. PERFORMING ORGANIZATION NAME(S) AND ADDRESS(ES) <br><br> Dept. of Earth and Atmospheric Sciences <br> St. Louis University <br> 3507 Laclede Avenue <br> St. Louis, MO 63103 | 8. PERFORMING ORGANIZATION REPORT NUMBER |
|---|---|

| 9. SPONSORING / MONITORING AGENCY NAME(S) AND ADDRESS(ES) <br><br> Air Force Research Laboratory <br> 29 Randolph Road <br> Hanscom AFB, MA 01731-3010 <br> Contract Manager: Katharine Kadinsky-Cade/VSBS | 10. SPONSORING / MONITORING AGENCY REPORT NUMBER <br><br> AFRL-VS-HA-TR-98-0039 |
|---|---|

| 12a. DISTRIBUTION / AVAILABILITY STATEMENT <br><br> Approved for public release; distribution unlimited | 12b. DISTRIBUTION CODE |
|---|---|

13. ABSTRACT *(Maximum 200 words)*

Pn and Lg spectra from the last eight Lop Nor explosions and many nearby earthquakes are collected from many broadband seismic stations, and analyzed to obtain source spectral characteristics and path Q. Pn spectra are unstable in amplitude with varying paths and source mechanisms. Much improvement has been made to stablize Pn spectral analysis. The main findings of this study include (1) Pn spectra from explosions have a spectral overshoot that is more significant than predicted by the theoretical source model used, (2) for explosions, Pn $M_0$ tends to be higher than Lg $M_0$; (3) for both Pn and Lg, $M_0$ scales with $f_c^{-\alpha}$, with $\alpha$ being close to 4 for explosions, and 3 for earthquakes; (4) for both explosions and earthquakes, at the same $M_0$ level, Pn $f_c$ are much higher than Lg $f_c$, and (5) for explosions, the significant spectral overshoot in Pn causes the Pn/Lg ratio to reach maximum around Pn $f_c$. This maximum is the dominant cause for that ratio to be significantly higher for explosions than for earthquakes in the frequency band of roughly 3 to 6 hz, a phenomenon previously reported for the same region.

| 14. SUBJECT TERMS <br> Pn, Lg, Q, source spectra, upper mantle structure, Central Asia, explosion discrimination | 15. NUMBER OF PAGES <br> 48 |
|---|---|
| | 16. PRICE CODE |

| 17. SECURITY CLASSIFICATION OF REPORT <br> Unclassified | 18. SECURITY CLASSIFICATION OF THIS PAGE <br> Unclassified | 19. SECURITY CLASSIFICATION OF ABSTRACT <br> Unclassified | 20. LIMITATION OF ABSTRACT <br> SAR |
|---|---|---|---|

# Contents

# SUMMARY

This report summarizes my research on spectral characteristics of excitation and propagation of Pn and Lg in the past year. Pn and Lg spectra from the last eight Lop Nor explosions and many nearby earthquakes are collected from many broadband IRIS, CDSN, Kyrghizstan and Kazakhstan network stations, and analyzed to obtain source spectral characteristics and path Q. Across the ten-station Kyrghizstan network, time domain Pn amplitude varies by as much as a factor of 19, despite the small aperture ($<$ 200 km) of the network. Spectral ratios of large, with respect to small, explosions are associated with a spectral overshoot that is more significant than predicted by existing theoretical models. Pn from earthquakes is further complicated by effects of non-isotropic radiation patterns. Several efforts are made to reduce the effect of these complexities in Pn spectral analysis. These include (a) the use of a moving-window average of spectra of Pn and its early coda, (b) a modification to the inverse method of Xie (1993) to tackle problems in Pn spectral inversion; (c) stacking spectra over similar, large explosions to obtain robust estimates of path Q; and (d) the use of multiple constraints on source spectra and path attenuation by combining Pn spectral inversion with analysis of inter-event and inter-station spectral ratios. The main findings of the analysis are: (1) for both explosions and earthquakes, the logarithm of seismic moments ($M_0$), estimated by inverting Pn and Lg spectra, scales with body wave magnitude ($m_b$) linearly, with slope of about 1.0, (2) for earthquakes, the $M_0$ estimated using Pn (Pn $M_0$) is similar to Lg $M_0$ at a given $m_b$ level, whereas for explosions, Pn $M_0$ tends to be higher than Lg $M_0$; (3) for both Pn and Lg, $M_0$ scales with $f_c^{-\alpha}$, with $\alpha$ being close to 4 for explosions, and 3 for earthquakes; (4) for both explosions and earthquakes, at the same $M_0$ level, Pn $f_c$ are much higher than Lg $f_c$ (by a factor of about 4 for earthquakes and 5 for earthquakes, respectively), (5) for explosions, the significant spectral overshoot in Pn causes the Pn/Lg ratio to reach maximum around Pn $f_c$. This maximum is the dominant cause for that ratio to be significantly higher for explosions than for earthquakes in the frequency band of roughly 3 to 6 hz, a phenomenon previously reported for the same region but with a more limited data base. This study thus reveals the cause of the Pn/Lg spectral ratio discriminant and more importantly, the limitation of our current theoretical framework for high-frequency regional wave excitations for both earthquakes and underground nuclear explosions.

# 1. INTRODUCTION

The seismic Pn and Lg wave trains are two of the most prominent regional phases on short-period records observed in continental areas. Beyond a critical distance (generally between 100 an 200 km), the Pn and Lg waves become the first and last main high-frequency regional phases to arrive, untangling themselves from other prominent regional phases such as Pg and Sn. The Pn wave can be modeled as an interference of multiple-diving waves, refracted at the Moho and traveling along the uppermost part of mantle (*e.g.*, Cerveny & Ravindra, 1971, Hill,1973). At closer distances, Pn is much like a pure head wave which evolves into mantle turning waves as distances increase (*e.g.*, Sereno & Given, 1990). At distances beyond about 12-13°, mantle turning waves are affected by the 420 and 670 km discontinuities and travel-time triplication occurs. Lg samples the continental crust and can be treated as a sum of higher mode surface waves (*e.g.*, Knopoff, 1973), or multiple supercritically reflected S waves (Bouchon, 1982). It can be observed at distances of up to a few thousand kilometers.

Both the Pn and Lg waves have been extensively used to study earth structure and seismic sources. In nuclear explosion seismology, they have each been used in magnitude determinations (*e.g.*, Nuttli, 1986a, 1986b, 1988; Vergino & Mensing, 1990). The amplitude ratios of P/Lg, including those of Pn/Lg, have been extensively used in studies of discrimination between explosions and earthquakes (*e.g.*, Blandford & Hartenberger, 1978; Blandford, 1981; Nuttli, 1981; Taylor *et al.*, 1988; Kim & Richards, 1993; Hartse *et al.*, 1997).

While the authors of the studies of P/Lg ratios generally agree that, at least in certain high-frequency bands, the P/Lg ratios from explosions tend to be higher than those from earthquakes, many questions still exist on when and why the P/Lg ratio can be used as an effective discriminant. For example, it is widely observed that the separation between Pn/Lg ratios from explosions and those from earthquakes varies with frequency, paths and source mechanisms in a complex manner (*e.g.*, Blandford, 1981; Chan *et al.*, 1991, Lynnes & Baumstark, 1991; Beckers *et al.*, 1993; Kim *et al.*, 1996). There appear to be cases in which Pn/Lg ratios observed for earthquakes fall into the explosion population. A more profound problem is that, even for the cases when the Pn/Lg ratio in certain high-frequency bands is known empirically to work as an explosion discriminant, there is a lack of understanding on why it works. Some possible mechanisms have been speculated on based on synthetics (*e.g.*, Evernden et al., 1986; Lilwall, 1988; Xie & Lay, 1994), but it is not practical to extensively verify these mechanisms until one can properly remove the path effects in the observed regional wave spectra, and obtain the spectral characteristics of source excitation. Such removal of path effects has been difficult and controversial (*e.g.*, Mueller & Cranswick, 1985; Harr *et al.*, 1986, Atkinson *et al.*, 1997; Haddon, 1997) and until recently, most studies on the P/Lg amplitude ratio discriminant have been conducted by measuring the ratios themselves; little attempt has been made to quantitatively infer spectral characteristics of the excitation of each phase (Pn and Lg) by each

1

source type (explosions and earthquakes), to see what might have been the systematic differences among these excitations that cause the discriminant to work.

Xie (1993) developed a non-linear algorithm to simultaneously invert for source spectral parameters, including seismic moment ($M_0$), corner frequency ($f_c$), and path $Q_0$ and $\eta$ (Q at 1 hz and its power-law frequency dependence, respectively) using seismic Lg waves from explosions. Advantages of that method include (a) it is an exhaustive search method, thus requiring no starting model for the unknown parameters, (b) it allows Lg Q to be path-variable, and (c) it is computationally fast due to a partitioning of model parameters, which allows $Q_0$ and $\eta$ to be estimated with linear regressions. Xie (1993), Xie et al. (1996) and Cong et al. (1996) applied that method to Lg spectra from many underground nuclear explosions and earthquakes in central Asia, recorded by many modern, broadband seismic stations in distance ranges of about 650 km to 4000 km. They obtained path $Q_0$, $\eta$ values that correlate well with major tectonic features, and Lg source $M_0$ and $f_c$ values for the numerous events. Based on these values and the respective values for $m_b$, the body wave magnitudes, they derived various scaling relations among these values to grossly quantify the spectral characteristics of excitation of Lg by explosions and earthquakes. Among the major discoveries that they made are: (1) for both source types the $\omega^{-2}$ models appeared to fit the Lg source spectra quite well, (2) the Lg $M_0$ correlates linearly with $m_b$ with slopes that are either close to, or slightly greater than, 1.0; (3) the Lg $M_0$ tends to scale with $f_c^{-\alpha}$, with $\alpha$ ranging from about 3.6 to 4.0; and (4) there appeared to be a tendency for the explosion $f_c$ to be higher than the earthquake $f_c$ at the same $M_0$ level, although there is also a considerable overlap between the two populations.

Recently, Xie (1998) presented a modification to the method of Xie (1993) to improve its stability in presence of random and systematic errors in the observed spectra, and successfully applied the modified method to the 1995 western Texas earthquake sequence ($M_w \sim 3.5$-$5.7$). In this report, we will extend the method of Xie (1993, 1998) to the spectral inversion of Pn waves to obtain estimates of path Pn $Q_0$ and $\eta$, and Pn source spectral characteristics. The latter include the $M_0$ and $f_c$ under the idealized $\omega^{-2}$ source models, and the possible deviation of the Pn source spectra from these models. We will apply the inverse method to Pn spectra from many seismic events in and around the Lop Nor Test Site (LTS) in Xinjiang, China. These include the last eight underground explosions detonated at the test site before September, 1996 (the time when the United Nations approved the Comprehensive Test Ban Treaty), and nineteen earthquakes that occurred between 1994 and 1996 in or near the LTS (Fig. 1). After 1992, the LTS became the only active land-based test site in the world, and has provided all of the new regional seismic signals from underground nuclear explosions. The large number of stations and high quality of records, as well as our new development of the methodology, enable us to derive grossly robust and reliable path corrections and source spectral parameters using Pn and Lg. In particular, for the first time we are able to derive the scaling between $M_0$

and $f_c$ estimated using Pn from underground nuclear explosions, and examine systematic deviations of Pn source spectra from the idealized $\omega^{-2}$ model. These put tight constraints on why the Pn/Lg spectral ratios may be be used as an explosions discriminant, and why the performance of this discriminant varies with frequenc y.

## 2. MODELING OF Pn SPECTRA

Street *et al.* (1975) were the first to model Lg wave spectra *via* a stochastic approach. Sereno *et al.* (1988) extended that modeling to the Pn wave. Here, we adapt the modeling of Sereno *et al.* and assume that $A_i(f)$, the Pn wave spectrum observed at an *i*th station, can be modeled as

$$A_i(f) = S(f)R(\theta_i)G(\Delta_i)\exp\left(-\frac{\pi f \Delta_i}{V_g Q_i(f)}\right)X_i(f)r_i(f) \ , \tag{1}$$

where $f$ is frequency, $\theta_i$, $\Delta_i$, $V_g$ and $Q_i(f)$ are the azimuth, distance, group velocity and quality factor of Pn from the source to the ith station. $R(\theta_i)$ is the non-isotropic source to Pn radiation pattern. $X_i(f)$ and $r_i(f)$ are, respectively, the site response and the effects of randomness. $S(f)$ is the isotropic component of the the Pn source spectrum, which is given by

$$S(f) = \begin{cases} \dfrac{M_0}{4\pi(\rho_s v_s \rho_c v_c^5)^{1/2}} \dfrac{1}{1 + f^2/f_c^2} & \text{for } earthquakes \\[4mm] \dfrac{M_0}{4\pi \rho_s v_s^3} \dfrac{1}{\left[1 + (1 - 2\beta)f^2/ f_c^2 + \beta^2 f^4/ f_c^4\right]^{1/2}} & \text{for } explosions \end{cases} \tag{2}$$

where $M_0$ and $f_c$ are seismic moment and corner frequency, $\rho_s$ and $v_s$ are source-zone density and P wave velocity, which in this study are set to be 2.6 $g/cm^3$ and 5.2 km/s for the explosions in the LTS, and 2.7 $g/cm^3$ and 6.5 km/s for the earthquakes (*e.g.*, Matzko, 1992; Li *et al.*, 1995). The latter values are also used for the crustal averaged density and P wave velocity, $\rho_c$ and $v_c$ (*e.g.*, Roecker *et al.*, 1993; Gao & Richards, 1994). In Eq. (2), we have used the omega-square model without overshoot for the earthquakes (often referred to as the "Brune's model") and the omega-square model with overshoot for the explosions (the modified Mueller-Murphy (M.M.M.) model; Sereno *et al.*, 1988), with $\beta$ being the parameter quantifying the amount of overshoot ($\beta$ is 0.75 for a Poisson medium). $G(\Delta_i)$ in Eq (1) is the geometrical spreading factor and takes the form

$$G(\Delta_i) = \Delta_0^{-1}(\Delta_0/\Delta_i)^m \tag{3}$$

where $\Delta_0$ is a reference distance, and $m$ is the decay rate of $A_i(f)$ at large distances ($\Delta > \Delta_0$). Typical values for $\Delta_0$ and $m$ are about 1 km and 1.3 to 1.5 for Pn, respectively, and are subjected to fairly large uncertainties (Sereno *et al.*, 1988; Sereno & Given, 1990). In this study we use an $m$ of 1.3 unless otherwise specified. $Q_i(f)$ in Eq (1) is the apparent Q (quality factor),

$$Q_i(f) = Q_{0i}\, f^{\eta_i} \qquad (4)$$

where $Q_{0i}$ and $\eta_i$ are Q to the $i$th station at 1 Hz and its power-law frequency dependence, respectively. Following Xie (1993), to develop a practical algorithm for the inversion of Pn spectra, we define $Q'_{0i}$ and $\eta'_i$ as the apparent Pn Q at 1 hz and its power-law frequency dependence, *via*

$$R(\theta_i)\exp\left(-\frac{\pi f^{1-\eta}\Delta_i}{V_g Q_{0i}}\right)X_i(f) = \exp\left(-\frac{\pi f^{1-\eta'}\Delta_i}{V_g Q'_{0i}}\right) \quad . \qquad (5)$$

With this definition, Eq (1) simplifies into

$$A_i(f_j) = S(f)G(\Delta_i)\exp\left(-\frac{\pi f_j^{1-\eta'}\Delta_i}{V_g Q'_{0i}}\right)r_i(f_j) \quad , \qquad (6)$$

where we have used subscript $j$ to indicate the $j$th discretized frequency. Equation (6) is a simplified, but practical stochastic modeling that relates the observed $A_i(f_j)$ to unknown source and path spectral parameters, defined by a model vector

$$m^T = = \left(M_0, f_c, Q'_{01}, \eta'_{01}, \ldots, Q'_{0N}, \eta'_{0N}\right)^T \quad , \qquad (7)$$

where $N$ is the number of stations recording the event, and the size of $m$ is $2N + 2$. From here on we will drop the superscript " ' " in $m$ and it is understood that estimates of $Q_{0i}$, $\eta_{0i}$ will be those of apparent Pn Q.

## 3. INVERSE METHOD

We now extend the non-linear method of Lg spectral inversion of Xie (1993, 1998) into the Pn spectral inversion. The inversion is event-based, with an objective to find an optimal model, $m$, that maximizes $\sigma_M(m)$, the posterior probability density function (Tarantola, 1987) which in our particular case, may be expressed as

$$\sigma_M(m) = const \times \rho_m(m) \times \exp\left\{-\sum_{i=1}^{i=N}\sum_{j=1}^{j=J(i)}\ln^2\left[r_i(f_j)\right]\right\} \quad , \qquad (8)$$

where $J(i)$ is the total number of frequencies available at the $i$th station, $r_i(f_j)$ is defined in Eq (6) and is calculable for any given set of observed $A_i(f_j)$ and model vector, $m$. $\rho_m(m)$ in Eq (8) is the marginal density function of apriori knowledge on the model. Assuming that we possess apriori knowledge on quantities $x_n$, (n=1,2,...), and that these quantities are statistically independent, we have

$$\rho_m(m) = \prod_n P_{x_n}(m) \quad , \qquad (9)$$

where $P_{x_n}(m)$ is the apriori knowledge on $x_n$ of the form

4

$$P_{x_n}(m) = \frac{1}{c_{n2} - c_{n1}} \left[ H(x_n - x_n^{aprior} + c_{n1}) - H(x - x_n^{aprior} - c_{n2}) \right] , \quad (10)$$

with $H(x)$ being a step function and $x_n^{aprior}$ being the apriori estimate of $x_n$. $(x_n^{aprior} - c_{n1}$, $x_n^{aprior} + c_{n2})$ defines an interval in which $x_n$ may take values with an equal probability. Examples of $c_{n1}$ and $c_{n2}$ are (a) they equal each other and approach zero, in which case $P_{x_n}(m)$ becomes a delta function and $x_n$ is precisely known, (b) $c_{n1}$ and $c_{n2}$ are the estimated error in the estimated $x_n^{aprior}$, and (c) $c_{n1}$ and $c_{n2}$ approach infinity and we have null apriori information on $x_n$. Examples of $x_n$ include (i) $f_c$, with $f_c^{aprior}$ estimated with the empirical Green's function approach; (ii) $\bar{Q}_0^{-1}$ and $\bar{\eta}$, the path-average of $Q_{0i}^{-1}$ and $\eta_i$:

$$\bar{Q}_0^{-1} = \frac{\sum_i \Delta_i / Q_{0i}}{\sum_i \Delta_i} , \quad (11)$$

$$\bar{\eta} = \bar{Q}_0 \frac{\sum_i \eta_i \Delta_i / Q_{0i}}{\sum_i \Delta_i} . \quad (12)$$

The search for optimal $m$ that maximizes $\rho_m(m)$ proceeds by a loop over all possible $M_0$, $f_c$ values for the event. In each loop, one first estimates the path $Q_{0i}$, $\eta_i$ values corresponding to the $M_0$, $f_c$ values using the relationship

$$-\frac{1}{\pi \tau_i} \ln \left( \frac{A_i(f)}{G(\Delta_i) S(f)} \right) = f^{1-\eta_i} / Q_{0i} + e_i(f) \quad , \quad i = 1, 2, 3, \ldots, I \quad (13)$$

where $e_i(f)$ is a small residual to be minimized. Once $Q_{0i}$ and $\eta_i$ are obtained, the complete set of model vector, $m$, is checked to see if it is consistent with the apriori knowledge in Eq (9). Only those $m$ that give non-zero values of Eq (9) are saved. After looping over all of the possible $M_0$, $f_c$ values, the residual squares (the term inside the exponential function in Eq (8)) saved for all $m$ that are searched in the loop, and give nonzero values of Eq (9), are brought together and compared. The model vector $m$ that gives the minimum residual squares (therefore maximum $\rho_m(m)$) is selected as the optimal solution. In practice, solving for Eq (13) requires a non-linear inversion *via* iterative procedure, which slows down the computation. Therefore, whenever the left-hand side of Eq (13) is not negative for all frequencies at the $i$th station, we take the logarithm of Eq (13) and fit $\log(Q_{0i})$ and $(1 - \eta_i)$ *via* linear regressions (*c.f.* Eq (18) and (19) of Xie, 1993), which greatly accelerates the computation.

## 4. DATA

The Pn data set used in this study consists of vertical component Pn waves from the last eight LTS underground nuclear explosions and nineteen nearby earthquakes, recorded by the broad-band IRIS stations AAK and BRVK, CDSN stations (for earthquakes only)

5

WMQ and LZH, Kazakhstan Network (KZNET; c.f. Kim et al., 1996) stations MAK, KURK and TLG, and the ten-station Kyrghizstan Network (KNET; Vernon, 1991). The explosions occurred between September 1992 and July, 1996, and earthquakes between 1994 and 1996. Before September, 1992 the station density in the area did not permit multiple-station recording of Pn at the proper distance range (roughly 200 km $\leq \Delta \leq$ 1300 km). Lg spectra from many of these events were not studied before, and are therefore also inverted in this study using the method of Xie (1993, 1998). The sampling rate of the instruments varies between about 20 per second (the broadband channels of IRIS and CDSN stations) and 100 per second (the high-gain channels of the KNET stations before late 1994). For explosions the CDSN stations do not provide data, making the minimum distances of data collection to be greater than about 790 km. For earthquakes, data from CDSN stations, including station WMQ, are available, resulting in a minimum distance of about 200 km. Between about 200 and 1300 km, the highest frequencies at which Pn spectra can be retrieved with sufficient signal/noise (S/N) ratios (> 2) are dependent on the events' size, and are typically between about 7 and 12 hz. For the Lg spectra recorded in the same distance range, the respective frequencies are somewhat lower (between about 5 and 10 hz). For Lg recorded at greater distances (between about 1,400 km and 2,700 km), the highest frequencies that yield sufficient (> 2) S/N ratios range are typically between about 1 and 5 hz. For both phases the lowest frequency available for our analysis is about 0.2 hz.

A striking feature of the Pn waves in the study area is the variability of their amplitudes: for the Lop Nor explosions, Pn amplitudes vary drastically with recording station within the Kyrghizstan Network, a ten-station network with a fairly small aperture (less than 200 km; Figure 2). Figure 3 shows an example of the explosion-generated record sections, where the time domain peak-to-peak Pn amplitudes vary by a factor of 19 between KNET stations KBK ($\Delta$ = 1173.7 km) and AML ($\Delta$ = 1277.5 km). Figure 4 shows the Fourier spectra calculated using the first 4.5 s of Pn in the time series plotted in Figure 3, with a 20% cosine-taper window. It is obvious that the amplitude variations in Pn spectra primarily occur at lower frequencies (~ 1 hz). For example, the amplitude ratio between stations KBK and AML is about 30 or greater between about 0.8 and 1.0 hz. Xie (1996) suggested that the most likely cause of the amplitude variation is some deep-seated 3D structural anomaly, such as a 3D Moho topography. In addition to amplitude variations of this kind, Pn amplitudes from earthquake sources often show some azimuthal variations that are not present in Pn from explosions. Specifically, for some earthquakes the ratio of Pn amplitudes at the western stations (e.g., the KNET stations and station TLG), with respect to those at stations in the north (stations MAK and KURK), are systematically lower than the respective ratios for the explosions.

These variations make it very difficult to conduct Pn spectral inversions using the stochastic model (Eq (6)) and the method described in the last section. To reduce the difficulty, for each seismogram containing Pn, we obtained the Fourier spectra with a series of 20% cosine taper windows that have a constant effective length of 4.5 s, but increase in

6

**Table 1.** Last Eight Lop Nor Explosions

| Event ID* | Origin Time(H:M:S) | $m_b$ | Location (°N, ° E) | No. of Stations† |
|---|---|---|---|---|
| 092592 | 07:59:59.9 | 5.0 | 41.763, 88.387 | 5 |
| 100593 | 01:59:56.6 | 5.9 | 41.667, 88.695 | 6 |
| 061094 | 06:25:57.8 | 5.7 | 41.527, 88.710 | 4 |
| 100794 | 03:25:58.1 | 5.9 | 41.662, 88.753 | 9 |
| 051595 | 04:05:57.8 | 5.7 | 41.603, 88.820 | 12 |
| 081795 | 00:59:57.8 | 5.5 | 41.587, 88.782 | 10 |
| 060896 | 02:55:57.7 | 6.0 | 41.657, 88.690 | 13 |
| 072996 | 01:48:57.8 | 4.9 | 41.824, 88.420 | 10 |

The origin times, locations and magnitudes are from the U.S. Geological Survey preliminary determination of epicenters (PDE) bulletin.

\* Event ID is composed of three groups of two-digit numbers, indicating the Month, Date and Year of the event, respectively.

† Number of stations that provided Pn spectra for this study.
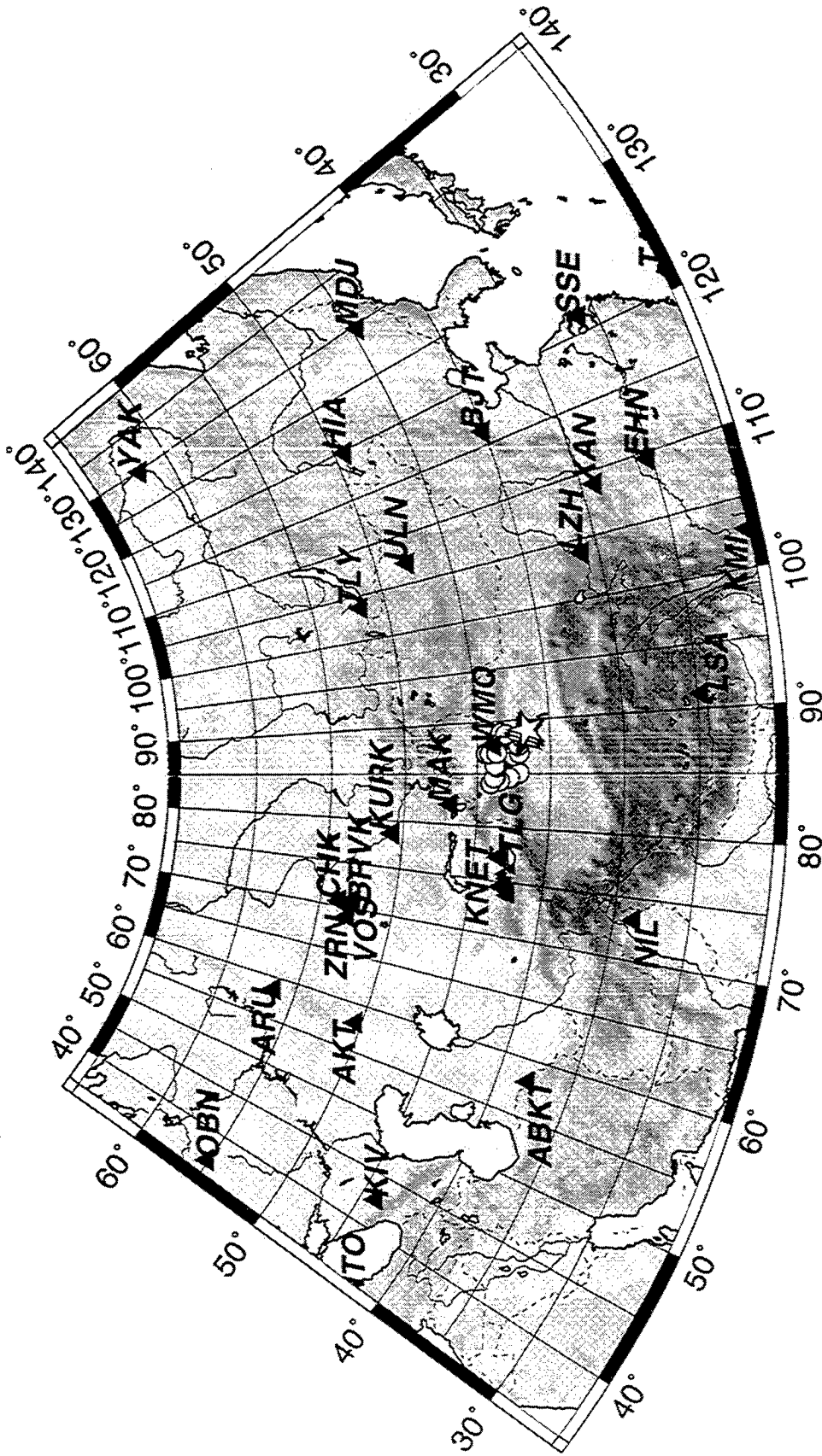
**Figure 1.** Map showing locations of Lop Nor Test Site explosions (stars), nearby earthquakes (circles) and seismic stations providing Pn and/or Lg waveforms used in this study.

8
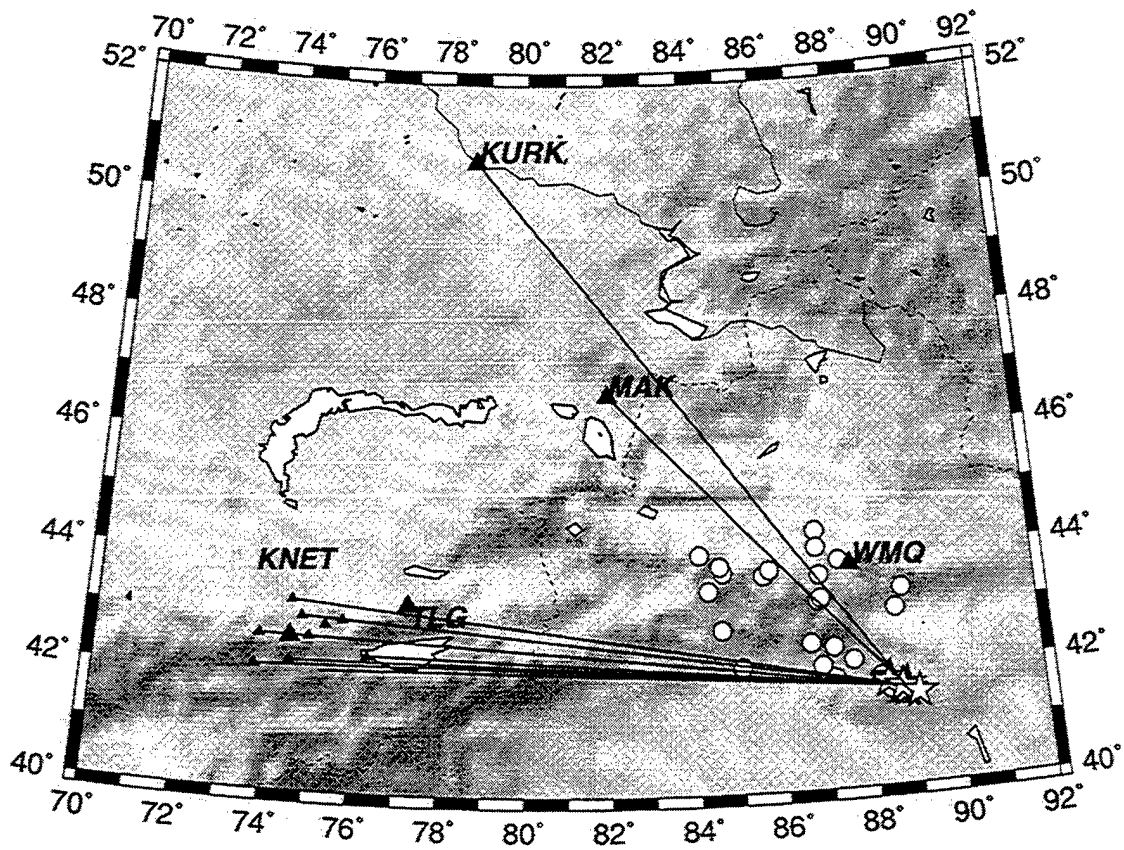
**Figure 2.** Detailed map showing locations of explosions and nearby earthquakes and seismic stations providing Pn waveforms. The great-circle paths are representative for Pn/Lg paths from explosions.

9
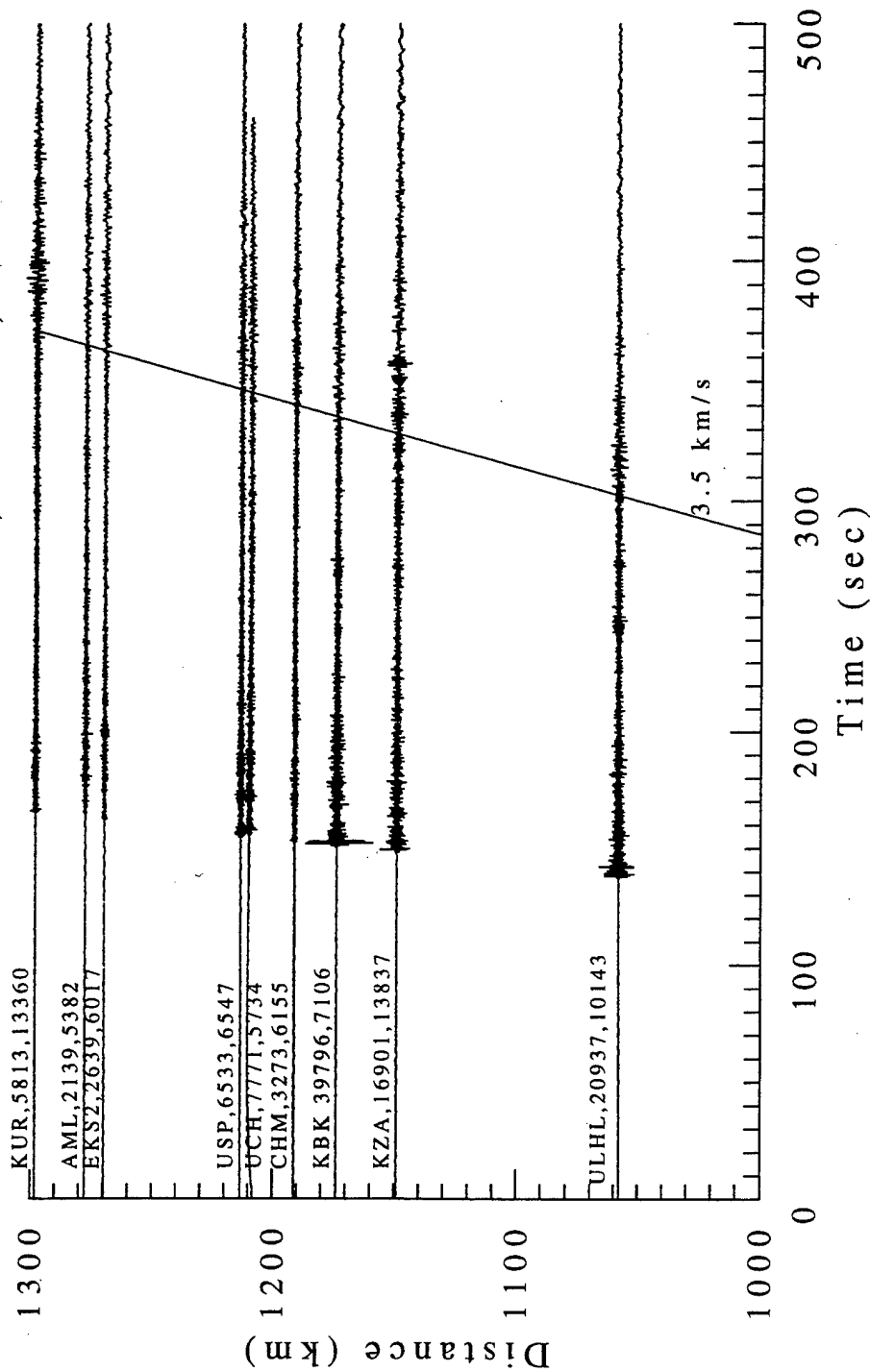
**Figure 3.** Record section showing seismograms in the distance range between 1061 and 1298 km, containing Pn and Lg from the 100794 explosion. The first arrival is Pn. The straight line marks the arrival of signal with a typical Lg group velocity (3.5 km/s). Numbers next to station codes are peak-to-peak Pn and Lg amplitudes in digital counts. Note Pn exhibits a large amplitude variation.
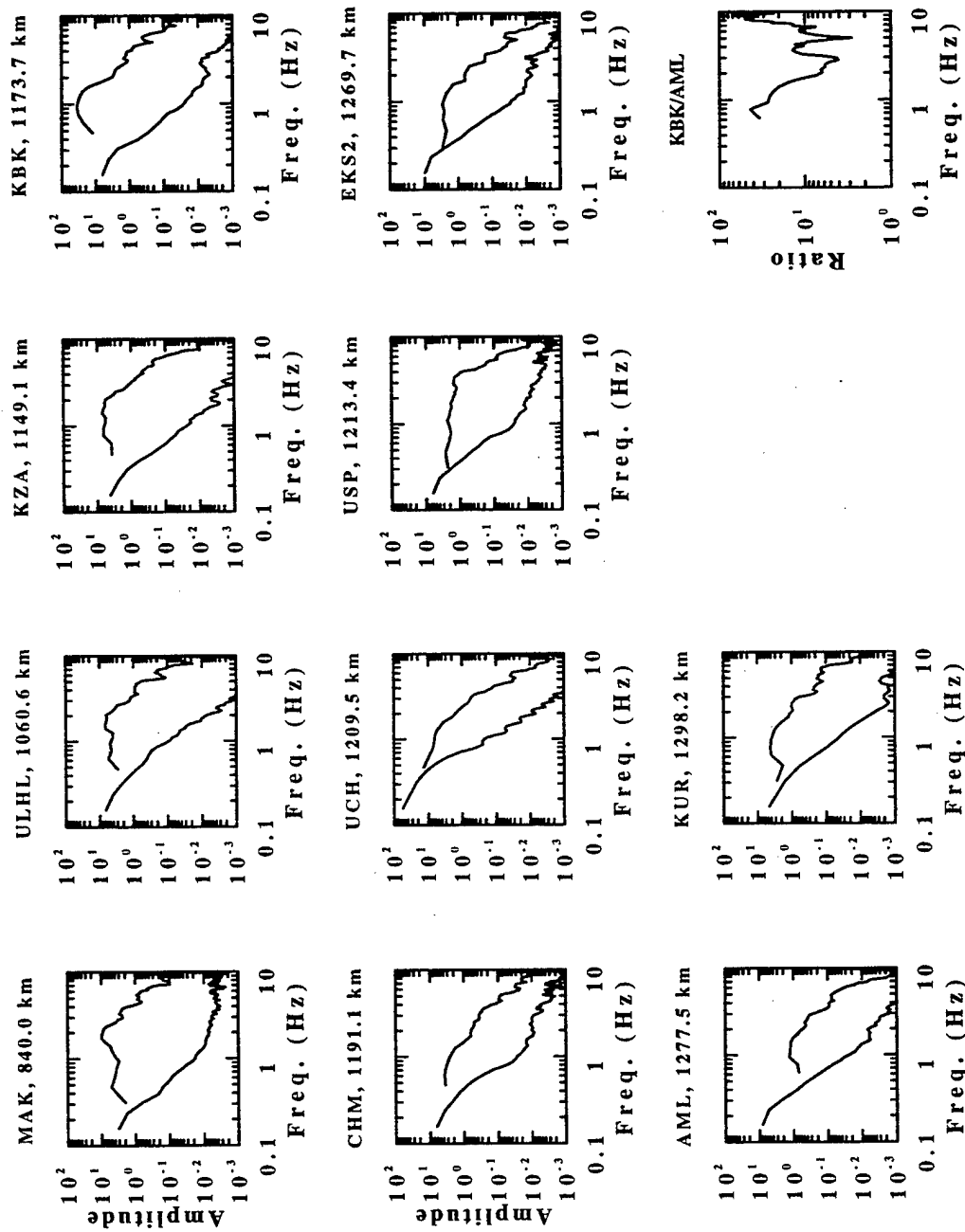
**Figure 4.** Fourier amplitude spectra of the first 4.5 s of Pn waves calculated using seismograms from explosion 100794 (Figure 3). Note the large amplitude variations near 1 Hz at varying stations. Panel in bottom right shows ratio of amplitude at KBK with respect to amplitude at AML.

event lapse time with a 50% overlap, to successively cover Pn and early Pn coda with group velocities $(V_g)$ greater than 6.6 km/s. These spectra are than averaged to reduce the amplitude variation associated with the onset of Pn. Averaged spectra from Pn and early Pn coda have been previously used by Zhu et al. (1991) to stablize the Pn spectral amplitudes, and are necessary in this study due to the large amplitude variations in the first few seconds of Pn. From here on we will refer to the averaged spectra of Pn and its early coda as "Pn spectra". The Lg records that are new to the present study are processed with the previously described procedure (Xie, 1993; Xie et al., 1996).

## 5. SPECTRAL ANALYSIS OF Pn

### § 5.1 Spectral ratios among Pn from explosions

The eight Lop Nor explosions are separated by a few tens of km or less (Table 1, Figure 2) and should have very similar path effect to permit an Empirical Green's function analysis (e.g., Li et al., 1995). Here we use the spectral ratios, rather than time domain deconvolution, to empirically remove the path effects and analyze the source behavior. From Eq (1), taking the ratio of Pn amplitude spectra at the same station from two colocated explosion events (I and II), we have

$$\frac{A_i^I(f)}{A_i^{II}(f)} = \frac{S^I(f)}{S^{II}(f)} \quad , \tag{14}$$

with the superscripts denoting the event. The right hand side of Eq (14) is the source spectral ratio which, under the M.M.M. model (Eq (2)), can be expressed as

$$\frac{S^I(f)}{S^{II}(f)} = \frac{M_0^I \left[ 1 + (1 - 2\beta)f^2 / f_c^{II^2} + \beta^2 f^4 / f_c^{II^4} \right]^{1/2}}{M_0^{II} \left[ 1 + (1 - 2\beta)f^2 / f_c^{I^2} + \beta^2 f^4 / f_c^{I^4} \right]^{1/2}} + \varepsilon(f) \quad , \tag{15}$$

where $\varepsilon(f)$ represents random, as well as systematic, deviations of the spectral ratio from that predicted by the M.M.M. model. Figure 5 shows the station-averaged spectral ratios among the eight explosions. There are two interesting features in these ratios: First, the events tend to form two groups, each having similar source spectra. One group of events consists of the two smaller $(m_b \sim 5)$ explosions (092592 and 072996), and the other one consists of the 5 to 6 larger $(m_b \sim 5.5\text{-}6.0)$ events. The second feature in Figure 5 is that the ratios of five large explosions $(M_b \sim 5.5\text{-}6.0)$, with respect to a small explosion (072996; $M_b = 4.9$), have a very pronounced overshoot near about 2 hz and undershoot near 4 hz. Under the M.M.M. model, Eq (14) and (15) relate the observed spectral ratios to the $M_0^I / M_0^{II}$, $f_c^I$ and $f_c^{II}$ values of the explosions through a non-linear relation, which allows us to invert for these values in a least-squares sense (i.e., by minimizing the L2 norm of $\varepsilon(f)$). We did such inversions by an iterative, linearized scheme, with the overshoot parameter, $\beta$, fixed at 1.0, a value that is larger than 0.75. The latter is the expected

12
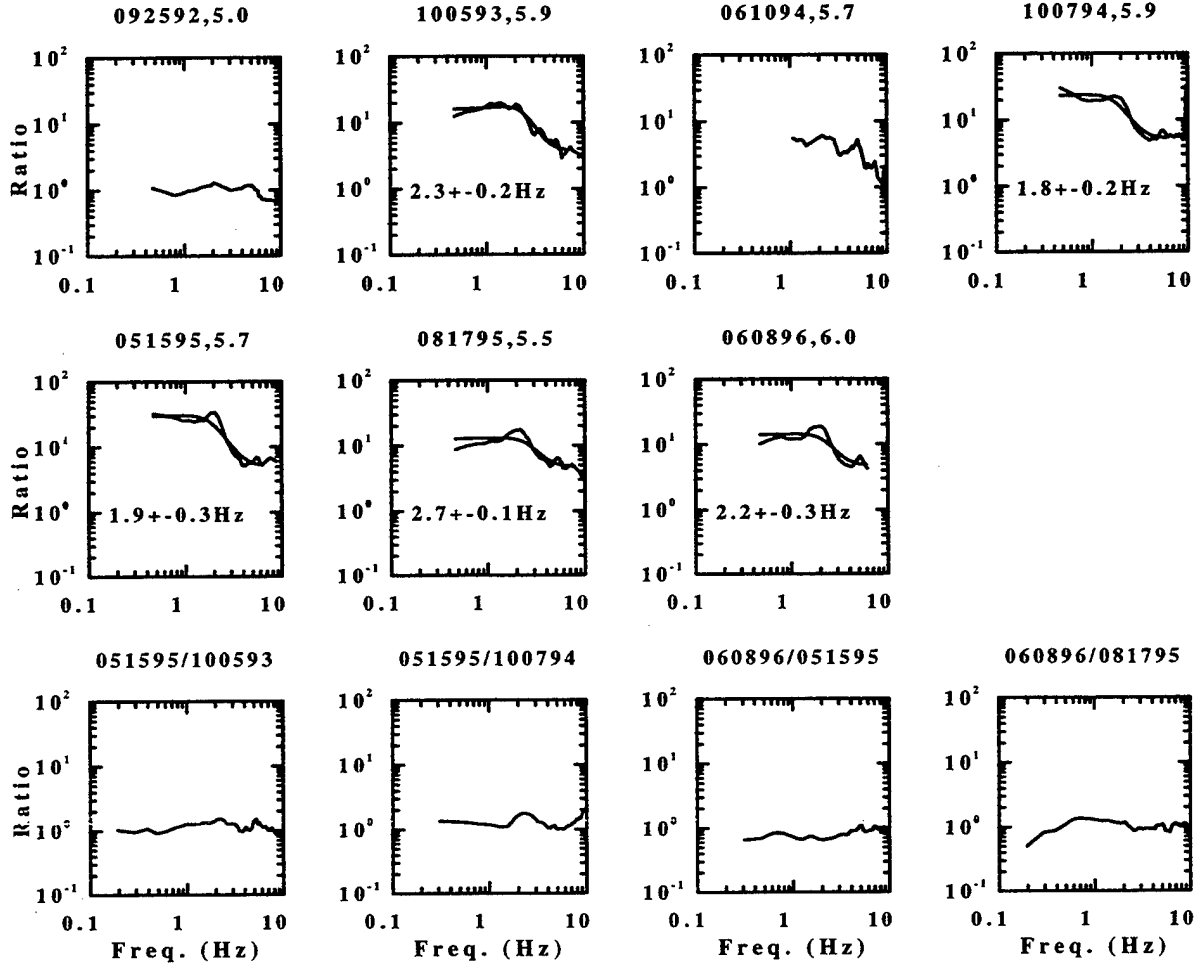
**Figure 5.** Ratios of amplitude spectra among Lop Nop explosions. Each panel is for a pair of two events for which, at each station, ratios of Pn spectra were calculated. These ratios are then averaged over all available stations to obtain the ratios plotted. The top two rows show ratios of seven of the eight explosions studied, with respect to the last explosion (072996, $m_b$ = 4.9). Smooth curves are theoretical ratios based on MMM model using inverted source parameters for five explosions (see text). Event ID and magnitudes are listed for the events whose spectra are used as numerator. Numbers inside the panels are the best fit $f_c^i$. Pn from event 061094 is recorded by only 4 stations and is excluded in the spectral ratio inversions. The bottom row includes spectral ratios for five larger events, with event IDs indicated on panel headers.

13

value for a Poisson medium, and is used for the Lg spectral inversion by Xie et al. (1996). The $M_0^I/M_0^{II}$ ratio and $f_c^I$, $f_c^{II}$ values obtained in the inversion are used to construct synthetic spectral ratios (smooth curves in Figure 4), which fit the overall trend of the observed spectral ratios, but underpredict the overshoot near 2 hz and the undershoot near 4 hz. This is because the M.M.M. model, even with the relatively large $\beta$ of 1.0, underpredicts the real overshoot in the source spectra near the source corner frequencies (near 2 hz for the larger explosions and 4 hz for event 072996, respectively).

### § 5.2 Estimate of Pn Q using the largest events

Since the Pn amplitude spectra are unstable with varying paths and sources, it is important to have robust inversions such that the resulting path Pn $Q_0$ and $\eta$ are similar for the 5 largest similar explosions (event 061094 is excluded here since only 4 stations recorded it and we are not confident to infer if it is similar to the other larger explosions). We experimented with inverting Pn spectra from each event separately, with an apriori knowledge of the form of Eq (9) and (10), such that $f_c$ are only permitted to take values between 1.0 hz and 3.5 hz. The latter range is from a conservative use of the apriori knowledge on $f_c$ obtained in the last section (1.8 to 2.7 hz, see Figure 5). In the inversions, we obtained path $Q_{0i}$ values that vary significantly. For example, the $Q_0$ value estimated to station AAK is about 300 when event 100593 is used, and above 700 when event 081795 is used. This indicates that the individual source spectrum deviates from the M.M.M. source model in an event-variable way, and the inversion is sensitive to these deviations, enough to cause the estimated model parameters to vary significantly among the similar events. To overcome such instability in model estimates, we averaged the Pn spectra among all, or a subset, of the five events. For each set of event-averaged spectra, we inverted for a single $m$, which is approximately the average model vector for events being averaged. Owing to the similarity of these events, this practice should result in robust and optimal estimates of Pn $Q_{0i}$, $\eta_i$ values. Figure 6 shows an example of such an inversion, in which the observed Pn spectra for 12 broadband stations are averaged over three events to obtain an $m$. Plotted in that figure are the Pn source spectra calculated using observed Pn spectra with path Q corrections, and the synthetic source spectra constructed using the $M_0$, $f_c$ obtained during the inversion. The overall fit, particularly for the station average (last panel), is good at high frequencies, and fairly good at lower frequencies, except that the synthetic source spectrum has less overshoot than the observed. This again shows that the M.M.M. model underestimates the level of spectral overshoot in the real Pn source spectra.

We changed the event composition in the averaging process by averaging two events that are not used in Figure 5, as well as by averaging all five events. In the respective inversions, the resulting path $Q_{0i}$ values to any station, such as AAK, differ by less than 10%. The $M_0$ values varied between 2.6 and $3.2 \times 10^{15}$ Nm, and $f_c$ values varied between 2.4 and 2.8 hz. We then separately inverted each of the five explosions again, by using a

14
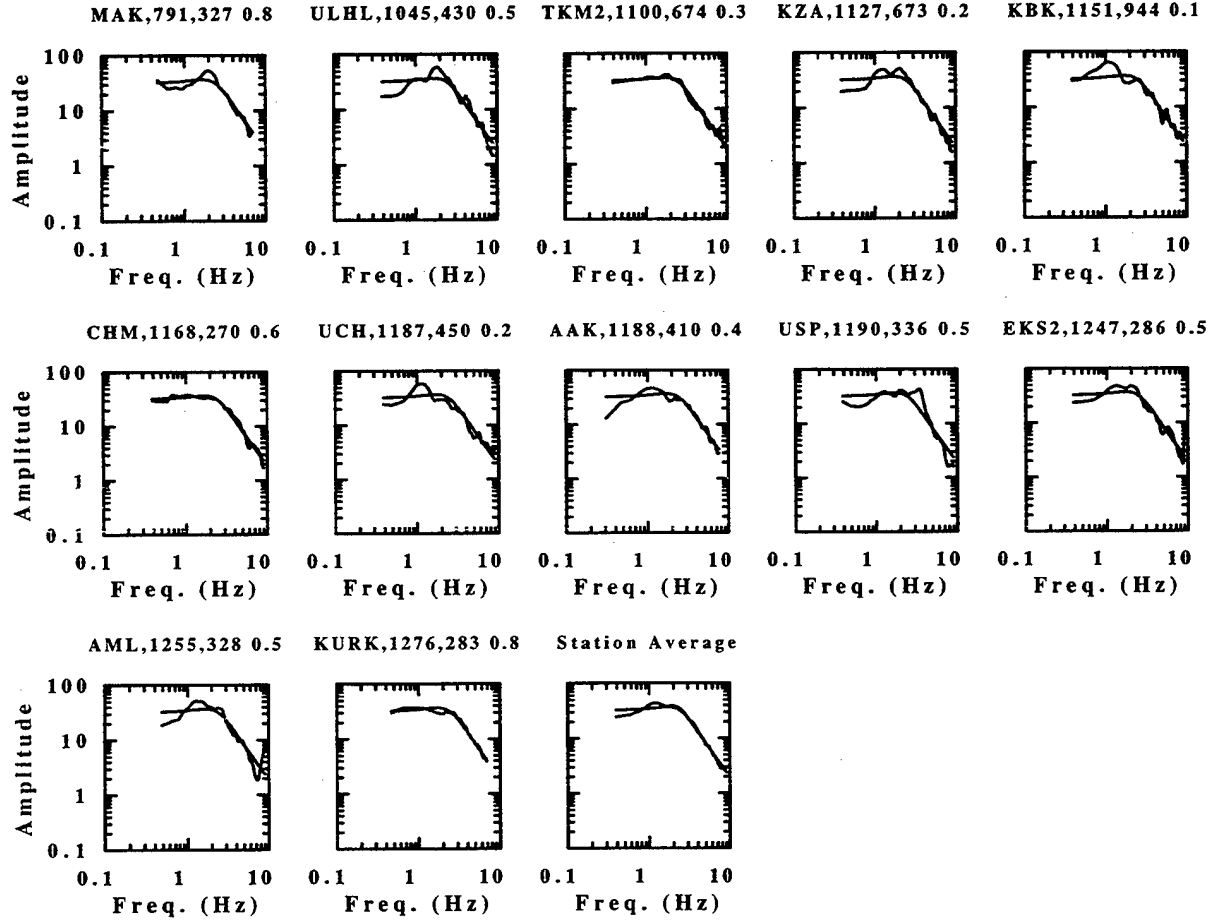
**Figure 6.** Averaged Pn source spectra for three explosions (100593, 100794 and 051595) at 12 stations. Fluctuating curves are observed Pn source spectra, obtained by first averaging Pn spectra over the three events, and then reducing these event-averaged spectra to source spectra by correcting for path effects. Path effects are estimated using $Q_{0i}$, $\eta_i$ values that are obtained by inverting event-averaged spectra. Smooth curves are synthetic source spectra, constructed using the MMM source model and event-averaged $M_0$ and $f_c$ values. The last panel shows station-averaged spectra.

apriori knowledge on path $Q_{0i}$ and $et_i$ to individual stations defined by

$$P_{Q_{0i}}(\boldsymbol{m}) = [H(Q_{0i}^{aprior} + 0.1 \times Q_{0i}^{aprior}) - H(Q_{0i}^{aprior} - 0.1 \times Q_{0i}^{aprior})] \qquad (16)$$

and

$$P_{\eta_i}(\boldsymbol{m}) = [H(\eta_i^{aprior} + 0.1) - H(\eta_i^{aprior} - 0.1)] \quad , \qquad (17)$$

where the $Q_{0i}^{aprior}$ and $\eta_i^{aprior}$ values are the average from the three inversions of the averaged spectra. Equations (17) and (18) permit the $Q_{0i}$ and $\eta_i$ to vary by no more than 10% and 0.1, respectively, from their apriori estimates. These new event-based inversions, with the apriori knowledge on $Q_{0i}$ and $\eta_i$, result in our final estimates of $M_0$ and $f_c$ values for the five largest explosions.

As indicated in the example in Figures 3 and 4, the estimated $Q_0$ and $\eta$ varies drastically across the KNET, due to the large amplitude variations mentioned before. The $\overline{Q_0}$ and $\bar{\eta}$ (path averaged $Q_0$ and $\eta$ values; Eq (11) and (12)) are, however, quite robust. For the eleven western stations, including the ten KNET stations and station TLG, $\overline{Q_0}$ and $\bar{\eta}$ are 364 and 0.5, respectively. For the two northern stations (MAK and KURK) $\overline{Q_0}$ and $\bar{\eta}$ are 303 and 0.7. For all paths the $\overline{Q_0}$ and $\bar{\eta}$ are 354 and 0.5, respectively, which maybe taken as the regional average. To see if the inversions might have been affected by the abnormal large amplitudes at stations KBK and KZA, we repeated the inversions without these two stations, and found that the resulting $Q_{0i}$, $\eta_i$ to other stations are unchanged.

To see whether the calculated $Q_{0i}$ and $\eta_i$, particularly their path-averaged values, are reasonable, we compared them with two estimates of path attenuation that are obtained separately. First, we measured the two-station $Q_0$ and $\eta$ between the two northern stations (MAK and KURK), using available Pn spectra from two explosions. These two stations are the only ones that we can find that (a) are well separated in $\Delta_i$ to permit a relatively stable measurement of Pn Q, (b) have similar azimuths; and (c) are relatively free of the afore-mentioned drastic amplitude variations among the western stations. We calculated the two-station spectral ratios from the two available events, and averaged these ratios to estimate the two-station $Q_0$ and $\eta$ (c.f. Xie & Mitchell, 1990). Figure 7 shows the result, where the calculated $Q_0$ and $\eta$ values are 277 ± 68 and 0.61 ± 0.05, which agree with, within the estimated uncertainties, the $\overline{Q_0}$ of 303 and $\bar{\eta}$ of 0.7 to the two stations (last paragraph). A second estimate of path attenuation is from Priestley and Patton (1997), who parameterized the time-domain peak-to-peak Pn amplitudes near station WMQ (Figure 1) as decaying with distance at a rate of $\Delta^{-1.47\pm0.26}$. At a distance of 1,100 km and using our modeling in Eq (1) or (6), with an $m$ (Eq (3)) of 1.3, that decay rate would correspond to a Pn $Q_0$ of 387, which is close to our estimate of $\overline{Q_0}$ of 354 for the entire study area. We are therefore assured that our $Q_{0i}$ and $\eta_i$ measurements, together with an $m$ of 1.3, are grossly adequate for the paths.

16
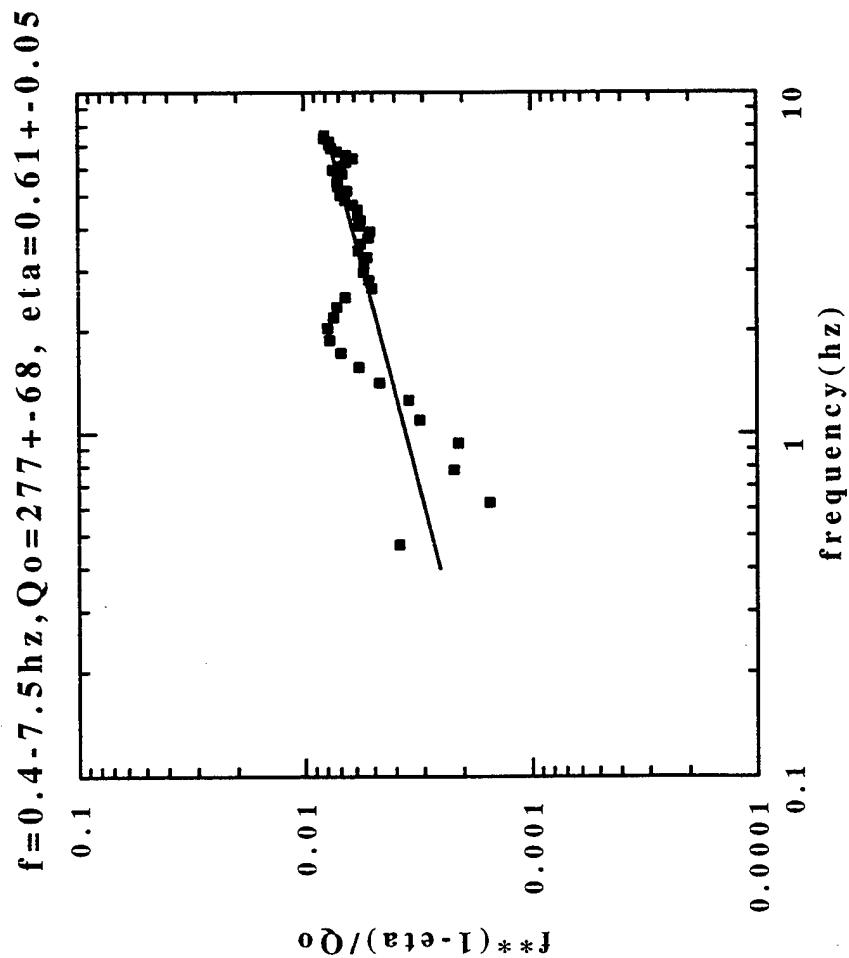
**Figure 7.** Event-averaged two station spectral ratios between stations KURK and MAK (the logarithm of $[A_1(f)G(\Delta_2)]$ divided by $[A_2(f)G(\Delta_1)]$, *c.f.* Xie and Mitchell, 1990), and the fitting for the optimal inter-station Pn $Q_0$ and $\eta$ (straight line). $G(\Delta_i)$ of the form of equation (3), with $\Delta_0$ of 1.0 km and m of 1.3, is used. The optimal $Q_0$ and $\eta$ values, together with their uncertainties, are indicated on the top. Only two explosions (100794, 051595) are recorded by the two stations simultaneously, and contributed to this plot.

## § 5.3 Sensitivity of the Pn Q estimates to the geometrical spreading model

The estimates of $Q_{0i}$, $\eta_i$ values in the last section are, of course, dependent on the geometrical spreading model assumed. We have chosen $m$ to be 1.3 since it is the value used in Scandinavia by Sereno et al. (1988), and approximates the value of 1.35 at the medium frequency used by Zhu *et al.* (1991) for eastern Canada. Xie (1996) computed extensive synthetics using a frequency-wave number integration code and the velocity models by Gao and Richards (1994), Roecker et al. (1993; model M1) and Quin and Thurber (1992), with the correction for the earth's curvature (Sereno and Given, 1990). Fitting the synthetic amplitudes between 0.2 and 2.5 hz by a frequency-independent geometrical spreading of the form of Eq (3), Xie (1996) estimated that the $m$ values ranged between 1.36 and 1.47, with considerable uncertainty (between 0.2 and 0.3). To see the effect of varying $m$ in the spectral inversion, we repeated the inversion using event-averaged Pn spectra with $m = 1.4$. The resulting $M_0$ and $f_c$ values remained unchanged, but $Q_{0i}$, $\eta_i$ values increased drastically. The $\overline{Q_0}$, $\bar{\eta}$ for all paths, for example, changed from 354, 0.5 to 748, 0.3, respectively. We conclude that the $Q_0$ and $\eta$ estimates in this study are valid only with a frequency-independent $m$ of 1.3, and may not necessarily represent the true quality factor in the uppermost mantle.

## § 5.4 Spectral inversions of Pn and Lg using apriori knowledge on path Q

Generally speaking, as compared to the five explosions studied in the previous sections, Pn spectra from the remaining three explosions and all of the earthquakes are more affected by complications such as fewer recording stations and/or lower S/N ratios and, in the case of earthquakes, significant radiation patterns. Spectral inversion of these events is therefore conducted by using the apriori knowledge on path-averaged $\overline{Q_0}$ and $\bar{\eta}$ (Eq (11) and (12)), which is derived using $Q_{0i}$, $\eta_i$ values obtained in the inversions of the five larger explosions. To use this knowledge, we employed Eq (10), with the respective $c_{n1}$ and $c_{n2}$ set at 0 (*i.e.*, with the right hand of Eq (10) taking the limiting form of a delta function). When Pn from the earthquakes are inverted, the use of the apriori knowledge on path-averaged $\overline{Q_0}$ and $\bar{\eta}$ caused individual $Q_{0i}$ and $\eta_i$ values to deviate significantly from the respective values estimated in the inversion of the five large explosions. For example, the $Q_{0i}$ values to the northern stations MAK and KURK, estimated during the inversion of Pn from earthquakes, are often systematically higher than those obtained by inverting the five large explosions, and just the opposite is found to the western stations (the KNET stations and station TLG). Lateral variations in Pn Q may have somewhat affected these deviations since the earthquake paths do not exactly overlap the explosion paths (Figure 2). The other likely cause for these deviations is the effect of the non-isotropic radiation pattern. Previous observations have suggested that Pn radiation pattern is a major factor which affects the observed amplitudes in various areas, including Iran, Northeastern U.S.A., and the study area (Nuttli, 1980; Zhao and Ebel, 1991, Xie, 1996).

18

Using the same methodology of Xie *et al.* (1996) and Xie (1998), we inverted the Lg spectra from five LTS explosions that are not studied by Xie *et al.* (1996), and the 19 earthquakes. When inverting the Lg from explosions, the overshoot parameter, $\beta$, was set at 0.75, which was used in Xie *et al.* (1996) and appears to fit the observed Lg spectra quite well. Figures 8 through 11 show the resulting $M_0$ and $f_c$ values for both phases (Pn and Lg) and source types (explosions and earthquakes), obtained in this and previous studies by Xie *et al.* (1996) and Cong *et al.* (1996).

## 6. SCALING BETWEEN $m_b$ AND $M_0$

Figures 8 and 9 show the body wave magnitude, $m_b$, versus $\log_{10}(M_0)$ estimated using Pn spectra in this study, as well as those estimated using Lg spectra in this and previous studies. For both source types and both phases, the logarithm of $M_0$ correlates with $m_b$ linearly, with slopes of about 1.0. We conducted linear regression analysis over the $m_b$ and $\log_{10}(M_0)$ values, and obtained the following relations:

$$\log M_0 = 9.53(\pm 0.51) + 1.16(\pm 0.09)\, m_b \quad \text{for } Pn \text{ from explosions,} \quad (18)$$

$$\log M_0 = 9.26(\pm 0.45) + 1.12(\pm 0.07)\, m_b \quad \text{for } Lg \text{ from explosions;} \quad (19)$$

$$\log M_0 = 10.79(\pm 0.48) + 1.00(\pm 0.10)\, m_b \quad \text{for } Pn \text{ from earthquakes;} \quad (20)$$

$$\log M_0 = 9.96(\pm 0.48) + 1.17(\pm 0.08)\, m_b \quad \text{for } Lg \text{ from earthquakes.} \quad (21)$$

An interesting feature of these figures and scalings is that for earthquakes, at any given $m_b$ level, the $M_0$ estimated using Pn ("Pn $M_0$") are similar to $M_0$ estimated using Lg ("Lg $M_0$"). Both Pn $M_0$ and Lg $M_0$ for earthquakes are higher than the Pn and Lg $M_0$ estimated for explosions at the same $m_b$ level. This is probably caused by the fact that, at a given moment level, the amplitudes of teleseismic P waves near 1 hz (the quantity used for $m_b$ determination) are systematically higher for explosions than for earthquakes.

Another interesting feature of the figures and scalings is that, for explosions, at any given $m_b$ level the Lg $M_0$ tend to be lower than the Pn $M_0$, although there is some overlap, making the trend weak. This trend is probably related to relatively low efficiency of Lg excitation by explosions, as compared to the efficiency of Pn excitation by explosions (Sereno *et al.*, 1988). This trend should not have been a dominant cause for the Pn/Lg spectral ratio discriminant since it is weak, and since it only causes the ratio to vary at low frequencies (< 1hz).

## 7. SCALING BETWEEN $M_0$ AND $f_c$

Figures 10 and 11 show the $f_c$ versus $M_0$ values obtained in this and previous studies. Linear regressions over the logarithm of these values yield the following relations:

$$\log M_0 = 18.34(\pm 0.65) - 4.73(\pm 1.2) \log f_c \quad \text{for } Pn \text{ from explosions;} \quad (22)$$
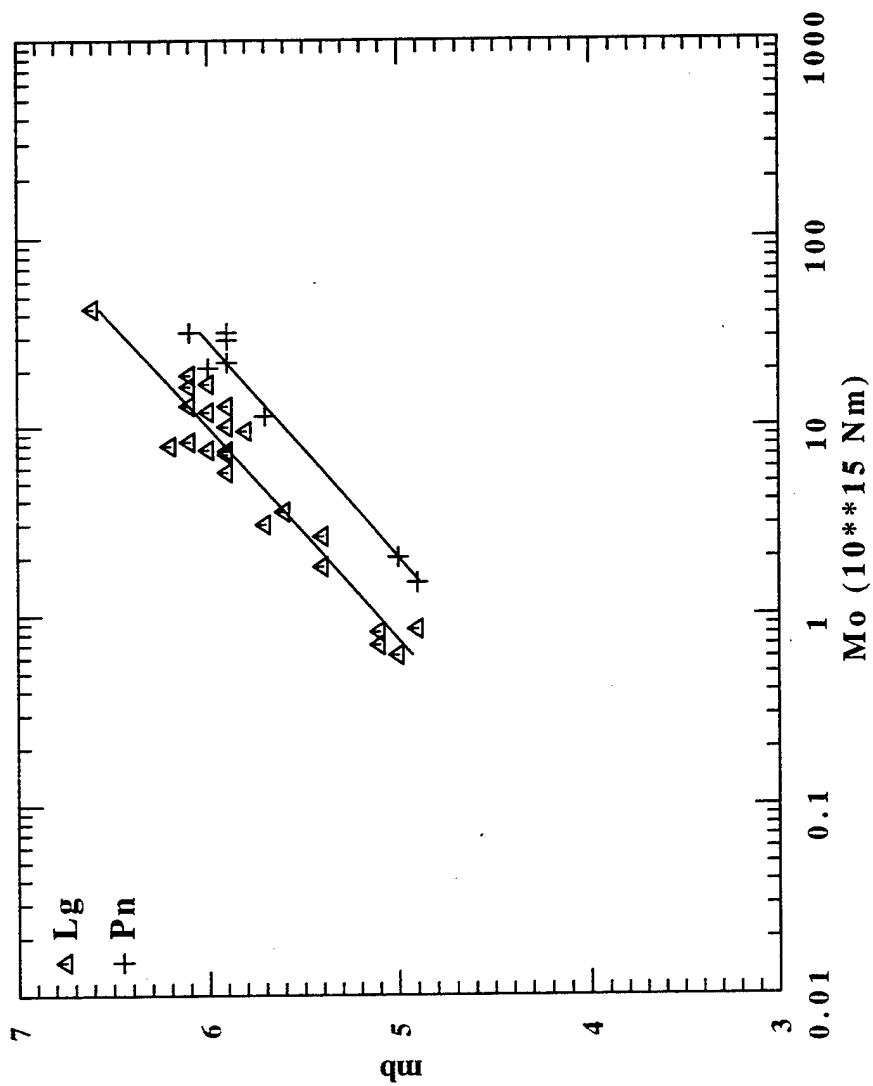
**Figure 8.** $m_b$ versus logarithm of $M_0$, estimated using Pn and Lg in this study and in Xie *et al.* (1996) for the explosions. Straight lines are the linear regression fit.
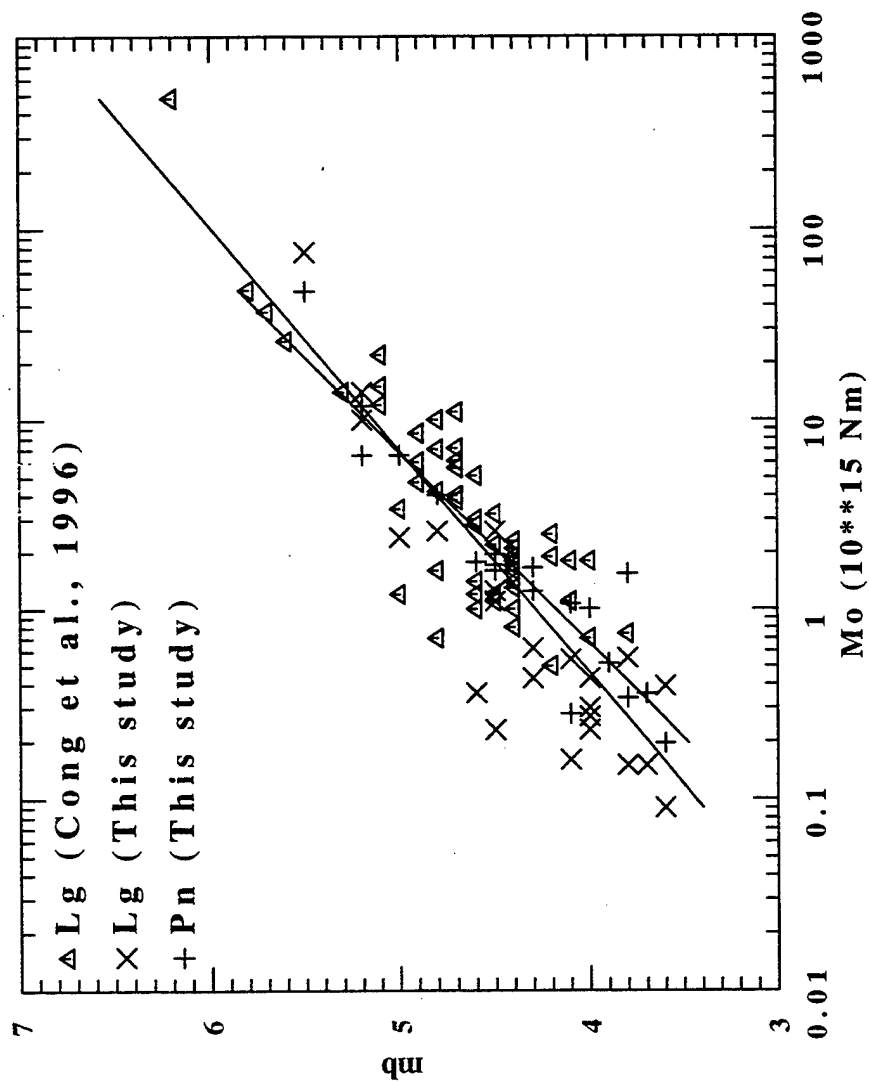
**Figure 9.** $m_b$ versus logarithm of $M_0$, estimated using Pn and Lg in this study and in Cong *et al.* (1996) for the earthquakes. Straight lines are the linear regression fit.

**Figure 10.** Logarithm of $M_0$ versus logarithm of $f_c$ values for the explosions, estimated using Pn and Lg in this and previous study. Straight lines are the linear regression fit.

**Figure 11.** Logarithm of $M_0$ versus logarithm of $f_c$ values for the earthquakes, estimated using Pn and Lg in this and previous study. Straight lines are the linear regression fit.

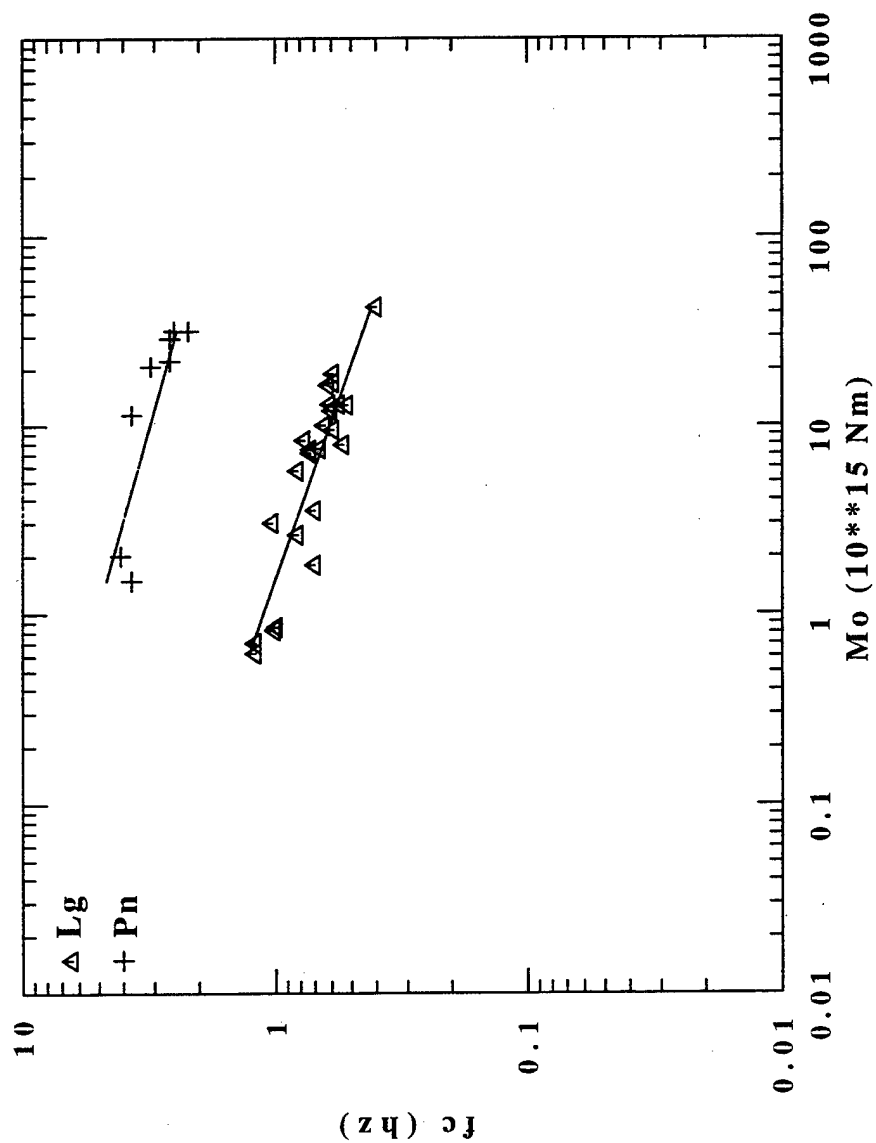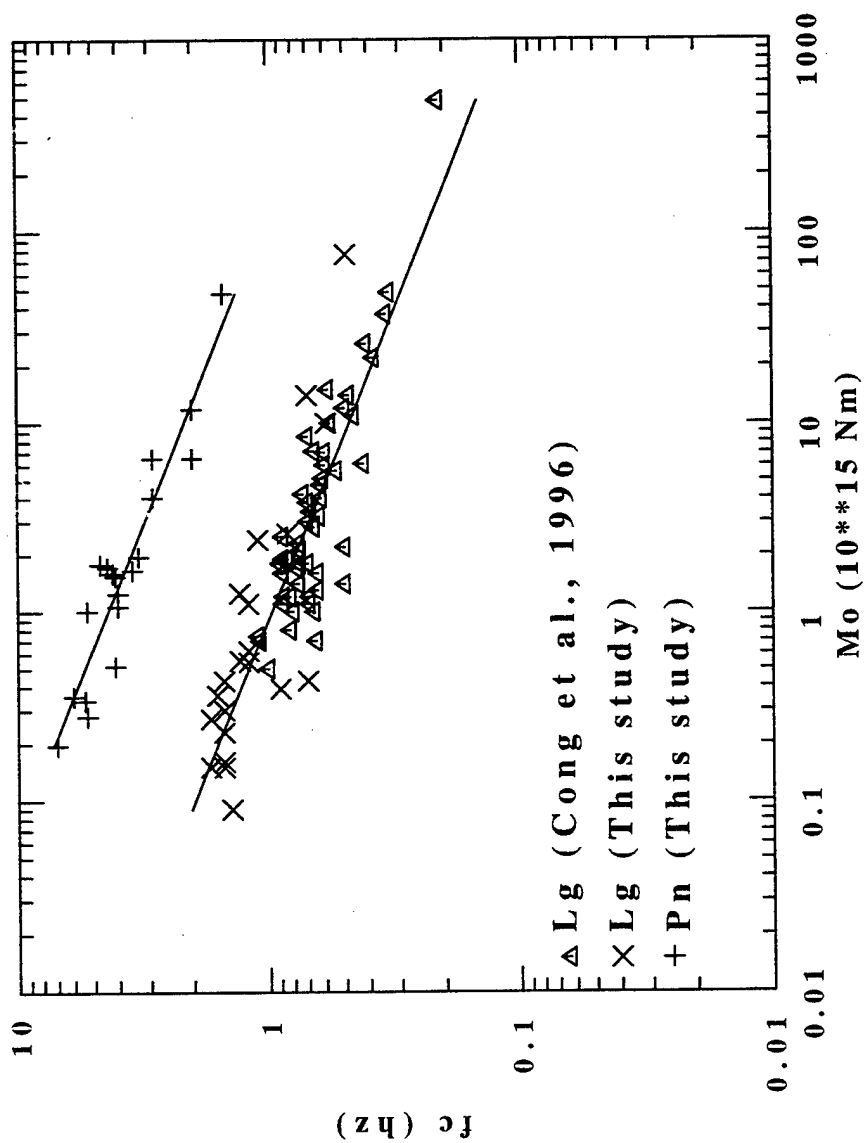$$\log M_0 = 15.18(\pm 0.23) - 3.81(\pm 0.39) \log f_c \qquad \text{for } Lg \text{ from explosions, (23)}$$

$$\log M_0 = 17.08(\pm 0.27) - 3.24(\pm 0.28) \log f_c \qquad \text{for } Pn \text{ from earthquakes. (24)}$$

$$\log M_0 = 14.96(\pm 0.33) - 3.25(\pm 0.21) \log f_c \qquad \text{for } Lg \text{ from earthquakes. (25)}$$

For Pn from explosions (Figure 10; Eq (22)), the intercept and slope are subjected to large uncertainties due to the small number of points (8 in total) available. Even with the uncertainties, however, we may conclude that the slopes of the above relations are generally between -3 and -4, with those developed using Pn and Lg from earthquakes being closer to -3, and those developed from explosions closer to -4.

The most interesting features in Figures 10 and 11 are that at the same $M_0$ level, Pn $f_c$ from both explosions and earthquakes tend to be much higher (roughly by a factor of 5) than the respective Lg $f_c$. For the explosions this is an rather expected phenomenon since there have been numerous studies reporting that the Pn/Lg ratios from explosions are higher than those from earthquakes at higher frequencies (*e.g.*, Blandford, 1981; Taylor *et al.*, 1988; Kim & Richards, 1993; Hartse *et al.*, 1997). If Pn $f_c$ from explosions are, but Pn $f_c$ from earthquakes are not, significantly higher than the corresponding Lg $f_c$, then we may conclude that this is the reason for the Pn/Lg spectral ratios to work at frequencies higher than the Lg $f_c$. What is rather unexpected is that Pn $f_c$ from earthquakes are also significantly higher (by a factor of about 4) than the corresponding Lg $f_c$ at a given $M_0$ level, say $10^{15} Nm$ (Figure 11; Eq (24) and (25)). In terms of $M_0$- $f_c$ scalings, the discrepancy between Pn $f_c$ and Lg $f_c$ from earthquakes mimics the similar discrepancy in Pn and Lg $f_c$ from explosions, and tends to make both types of sources similar in terms of $M_0$ - $f_c$ scaling. For earthquakes, the amount that the Pn $f_c$ offsets the Lg $f_c$ at the same $M_0$ level is about 4, which is slightly less than the respective offset for explosions (about 5). But this slight difference does not seem to be sufficient to cause the Pn/Lg ratio to work as an explosion discriminant at higher frequencies. It seems that the Pn/Lg spectral ratio discriminant can not be explained by a difference in $M_0$ - $f_c$ scalings for different source types.

## 8. CAUSE OF THE Pn/Lg RATIO DISCRIMINANT

The scalings developed in the last section enable us to predict, subject to some uncertainties, generic source spectra for each types of sources (earthquakes and explosions) and phase (Pn and Lg), at any given $m_b$ level. Figure 12 shows such predicted, "generic" source spectra for each type of source and phase, at the end $m_b$ levels of this study (*i.e.*, the minimum and maximum $m_b$ for each population in Figures 8 and 9). The ratios between the generic Pn/Lg source spectra are also calculated and plotted in Figure 12. If in the observed data there is a tendency for the Pn/Lg spectral ratio to be higher for explosions at certain frequency band, we ought to be able to reproduce that tendency, or the derivation of the scalings will have been incorrect.
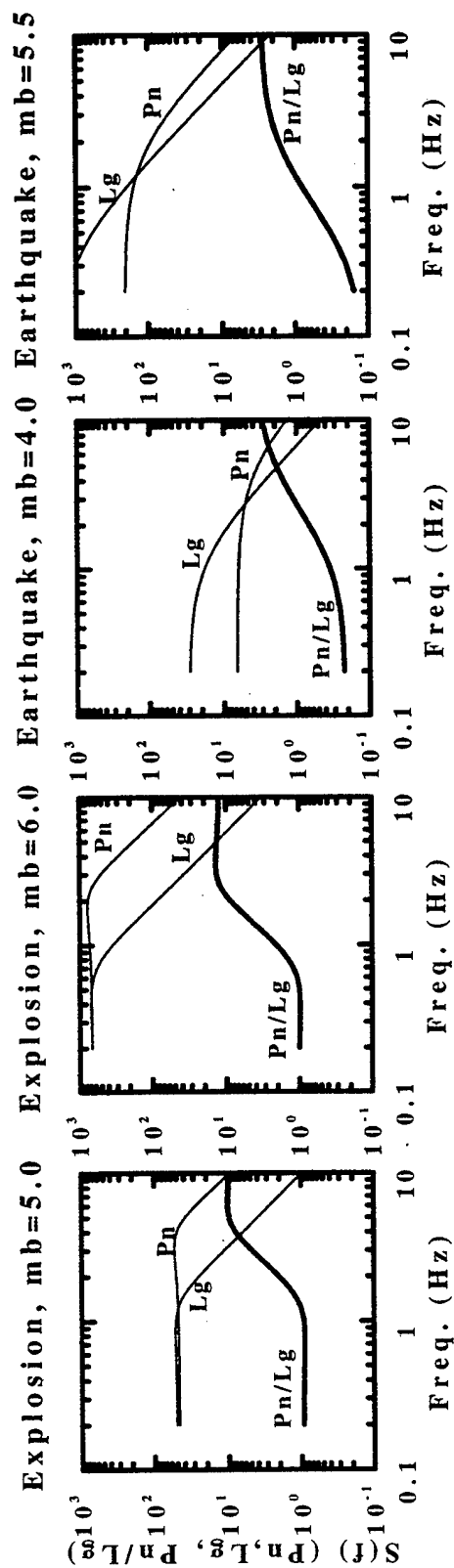
**Figure 12.** Generic Pn and Lg source spectra (thin curves) constructed for hypothetical explosions and earthquakes with the end $m_b$ levels in Figures 8 and 9. The spectra are constructed using the scalings derived in this study (equations (18) through (25)), and the theoretical, M.M.M. source model (equation (2); SI unit). Also plotted are the Pn/Lg ratios (thick curves) derived from the source spectra.
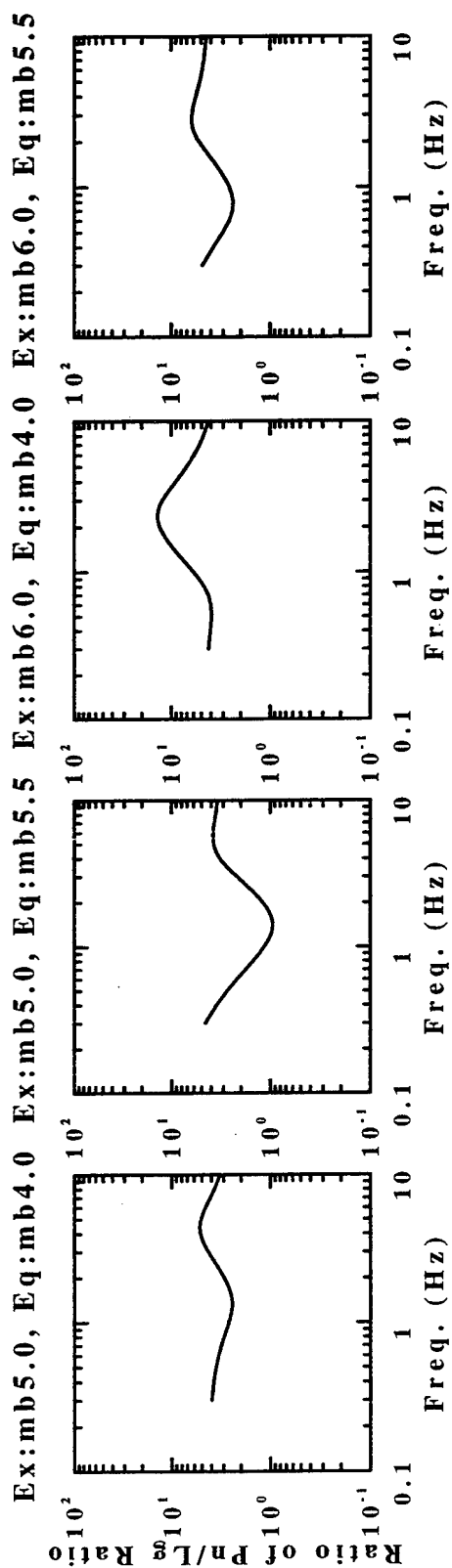
Figure 13. Ratios among Pn/Lg ratios in Figure 12.

26

Above 1 hz, the Pn/Lg spectral ratios in Figure 12 all increase with increasing frequency. The manner of the increase, however, is different for explosions and earthquakes. For an explosion, the generic Pn/Lg ratio increases more rapidly in the frequency range between the Pn $f_c$ and Lg $f_c$, and reaches a maximum near the Pn $f_c$ due to the Pn spectral overshoot. In contrast, the generic Pn/Lg spectral ratios for earthquakes increase more slowly between Pn $f_c$ and Lg $f_c$, and no maximum is reached until about 10 hz. As a result, the generic Pn/Lg ratios for explosions tend to be higher than those for earthquakes near the Pn $f_c$. This can be more clearly seen in Figure 13, where generic Pn/Lg ratios for explosions are divided by those for earthquakes, resulting in "ratios of Pn/Lg ratios", which directly reflect the difference between the generic explosion Pn/Lg spectral ratios and the generic earthquake Pn/Lg ratios. All of the ratios of ratios in Figure 12 reach maximum near the explosion Pn $f_c$ (between about 2.5 and 5 hz). This is highly consistent with the previous observation of Pn/Lg and Pg/Lg ratio in the study area by Hartse et al. (1997), who concluded, based on spectra collected from stations AAK and WMQ, that the maximum separation between P/Lg ratios from explosions and those from earthquakes occurred in a frequency band between about 3-6 hz. Thus the result of this study is that the Pn/Lg spectral ratio from explosions are significantly higher than those from earthquakes in a frequency band spanned by the Pn $f_c$ from explosions, mainly due to the significant spectral overshoot of Pn excited by explosions. We recall that analyses in two previous sections have indicated that the theoretical source model used in this study (the M.M.M. model) underestimates the amount of spectral overshoot in the observed Pn from explosions. Therefore, in Figures 12 and 13 we have likely underpredicted the observed difference between Pn/Lg spectral ratios from explosions and those from earthquakes. In other words, in the observed Pn, the spectral overshoot plays even more significant role in raising the Pn/Lg spectral ratios from explosions relative to the Pn/Lg spectral ratios from earthquakes.

## 9. SOFTWARE DEVELOPMENT

The computer software developed during the last year includes:

1. Program "nl" which takes observed data of up to about 10,000 points, any nonlinear relationship that relates these data points to up to 10 model parameters, and finds the model parameters that best fit the data in a least squares sense. The finding of the best model parameters is achieved by a Newton-like, iterative scheme. This program can be expanded into finding model parameters that have larger size, with more data points, with minimal effort.

2. Program "motion" which generates expected Pn or Lg ground motion for a given type and magnitude of the hypothetical seismic event (explosion or earthquake), using appropriate source spectral model, path Q, and source spectral scalings (i.e., scalings among $m_b$, $M_0$ and $f_c$).

# 10. CONCLUSIONS AND DISCUSSION

Pn and Lg spectra from the last eight Lop Nor Test Site (LTS) explosions and nineteen nearby earthquakes are collected from many broadband stations in the Republics of Kyrghizstan, Kazakhstan and China (earthquakes only). Pn from explosions show drastic amplitude variations (by a factor of about 20 to 30 in time and frequency domains) across the Kyrghizstan network, which is located about 1060 to 1280 km west of the LTS. Pn amplitudes from earthquakes are further complicated by variations that are not only associated with lateral variations of apparent Pn Q, but non-isotropic source radiation patterns. Various methods have been used in this study to improve the reliability in extracting the spectral characteristics of source excitation and path attenuation from the observed Pn spectra. We used average spectra of Pn and its early coda instead of the first few seconds of Pn for the analysis. Averaging processes have also been extensively used to reduce fluctuations in inter-station and inter-event spectral ratios, which lead to strong constraints on Pn source spectra and path Q. The path-averaged Pn $Q_0$ and $\eta$ (Pn Q at 1 hz and its power-law frequency dependence, respectively) are obtained by inversions of event-averaged spectra among five large and similar explosions, and are used as apriori knowledge for inversions of other events. The improved methodology, as well as the large number of available stations, enable us to invert for source seismic moments ($M_0$) and corner frequencies ($f_c$) using the observed Pn spectra and a stochastic model of Pn excitation and propagation. Our analysis demonstrated that Pn source spectra from explosions contain a spectral overshoot that is more significant than predicted by the theoretical, modified Mueller-Murphy source model, and than the overshoot in explosion-excited Lg. We also demonstrated that in the study area, the estimation of Pn $Q_0$ and $\eta$ values are highly dependent on the geometrical spreading models used.

In addition to analyzing Pn spectra, we also inverted Lg spectra from the explosions and earthquakes. Various scalings have been developed among the body-wave magnitude ($m_b$), $M_0$ and $f_c$ values estimated using both Pn and Lg, from both explosions and earthquakes. As expected, the logarithm of $M_0$ values correlates with $m_b$ linearly, with slopes close to 1.0. The $M_0$ tend to scale with $f_c^{-\alpha}$, with $\alpha$ being close to -3 for Pn and Lg from earthquakes, and -4 for Pn and Lg from explosions. One of the most surprising discoveries of this study is that for both explosions and earthquakes, at a given $M_0$ level, the $f_c$ values estimated using Pn are significantly higher than the $f_c$ values estimated using Lg for both explosions and earthquakes. The offset of Pn $f_c$ from Lg $f_c$, at the same $M_0$ level, is about a factor of 4 and 5 for earthquakes and explosions, respectively.

Previously, it has been reported that the observed Pn/Lg ratios from explosions often tend to be higher than those from earthquakes; the difference is maximized in limited high frequency ranges (3-6 hz for the study area). Through the examination of the generic spectral ratios that were computed using the various scaling relationships and the theoretical model used in this study, we found that the dominant cause for the frequency-variable

28

difference between explosion-generated Pn/Lg ratio and earthquake-generated Pn/Lg ratio is the significant spectral overshoot in explosion-generated Pn spectra. That effect was clearly seen in the generic Pn/Lg ratios, but should be even more significant in the observed Pn/Lg ratios since the generic Pn/Lg ratios under-predict the effect of the Pn spectral overshoot for explosions, a limitation resulting from the modified Mueller-Murphy source model.

The amount of Pn spectral overshoot from underground nuclear explosions is likely underpredicted by currently available theoretical source spectral models other than the modified Mueller-Murphy model. More work is needed to improve these models. The theoretical, stochastic models for Pn propagation and attenuation are also limited in that they can not precisely predict the effects of complicated velocity structure. We have demonstrated that even a small amount of error in the geometrical spreading model can cause a large change in the estimated Pn $Q_0$ and $\eta$ values. The estimated Pn $Q_0$ and $\eta$ values, even when averaged over many paths, do not necessarily represent the true quality factor of the Earth's uppermost mantle.

At individual stations, the observed Pn spectra are highly affected by the 3D earth velocity structure. The unstable path effects, as well as the non-isotropic source radiation patterns of earthquake sources, make Pn spectral amplitudes highly unstable. Consequently, the Pn/Lg spectral ratios are highly dependent on the path and event focal mechanism. The use of average spectra of Pn and early Pn coda may reduce, but not eliminate, this complication. In the worse-case scenario, variations in Pn/Lg ratios, caused by varying effects of path propagation and and source radiation pattern, may overwhelm the difference in the Pn/Lg source spectral ratios caused by varying source types. Careful calibration of path effects and increasing station density are necessary for successful discrimination of explosions from earthquakes if the spectral ratios of Pn and early Pn coda, with respect to Lg, are to be used.

The findings of this study, including the dominant cause of the frequency-varying performance of the Pn/Lg spectral discriminant, is limited by the limited ranges in epicentral distance (> 800 km for explosions), frequency (usually between about 0.2 and 8 to 10 hz), and magnitude (4.0 to 5.5 for earthquakes and 5.0 to 6.0 for explosions). It is also limited by the use of only two regional phases (Pn and Lg). It will be important to extent the analysis to Pn/Lg observed for other ranges of distance, frequency and magnitude, which may require data sets that are collected from a different geographic region. Other important future work will be to extend the analysis to other regional waves, such as Pg, whose ratio with Lg has been empirically suggested as being a more robust discriminant between explosions and earthquakes for the study area (Hartse et al., 1997).

# REFERENCES

Atkinson, G.M., Boore, D.M. and J. Boatwright. 1997. Comment on "Earthquake source spectra in eastern North America" by R.A.W. Haddon, *Bull. Seimo. Soc. Am.*, **87**, 1697-1702.

Beckers, J., S. Schwartz and T. Lay, 1993. Analysis of the effects of Eurasian crustal and upper mantle structure on regional phases using broadband seismic data, *Phillips Laboratory Final Report*, PL-TR-93-2131, 94 pp., ADA272446.

Blandford, R.R. and Hartenberger, R.A., 1978. Regional discrimi nation between earthquakes and explosions *(abstract), EOS, Trans. Am. Geophys.*, **59**, 1140.

Blandford, R.R., 1981. Seismic discrimination problems, *NATO Advanced Study Institutes Series C*, Mathematical and Physical Sciences, 695-740.

Bouchon, M., 1982. The complete synthesis of seismic crustal phases at regional distances, *J. Geophys. Res.*, **87**, 1735-1741.

Cerveny, V. and R. Ravindra, 1971. *Theory of Seismic Head Waves*, University of Toronto Press, 312 pp.

Chan, W.W., Baumstark, R. and Cessaro, R.K., 1990. Spectral discrimination between explosions and earthquakes in central Eurasia. *Phillips Laboratory Annual Scientific Report*, GL-TR-90-0217:1-38, ADA230048.

Cong, L., J. Xie and B.J. Mitchell, 1996. Excitation and propag ation of Lg from earthquakes in Central Asia with implications on explosion/earthquake discrimination, *J. Geophys. Res.*, **101**, 27779-27810.

Evernden, J., Archambeau, C. & Cranswick, E., 1986. An evaluation of seismic decoupling and underground nuclear monitoring using high-frequency seismic data, *Rev. Geophys.*, **24**, 143-215.

Gao, L. & Paul G. Richards, 1994. Studies of Earthquakes on and near Lop Nor, China, Nuclear Test Site, in *Proc. 16th Annual Seismic Research Symposium, 7-9 September 1994*, Phillips Lab, Hanscom AFB, Massachussetts, 311-317, PL-TR-94-2217, ADA284667.

Haddon, R.A.W., 1997. Reply to Comment by G.M. Atkinson et al. on "Earthquake source spectra in eastern North America" by R.A.W. Haddon, *Bull. Seimo. Soc. Am.*, **87**, 1703-1708.

Harr, L.C., C.S. Mueller, J.B. Fletcher, and D.M. Boore, 1986. Comments on "Some recent Lg phase displacement spectral densities and their implications with respect to prediction of ground motions in Eastern North America" by R. Street, *Bull. Seism. Soc. Am.*, **76**, 291-295.

Hartse, H.E., S.R. Taylor, W. S. Phillips and G.E. Randall, 1997. A preliminary study of regional seismic discrimination in central Asia with emphasis on western China, *Bull. Seismol. Soc. Am.*, **87**, 551-568.

Hill, D., 1973. Critically refracted waves in a spherically symmetric radially heterogeneous earth model, *Geophys. J. R. astr. Soc.*, **34**, 149-177.

Kim, W.-Y. & Richards, P.G., 1993. Discrimination of earthquakes and explosions in the Eastern United States using regional high-frequency data, *Geophys. Res. Lett.*, **20**, 1507-1510.

Kim, W.Y., G.L. Vsevolozhsky, T.L. Mulder & P.G. Richards. 1996. Practical analysis od seismic activity in northwestern China during September 4-7, 1995, in *Proc. 18th Annual Symposium on Monitoring a Comprehensive Test Ban Treaty, 4-6 September 1996*, edited by J.F. Lewkwicz, J.M. McPhetres and D.T. Reiter, Phillips Lab, Hanscom AFB, 735-744. PL-TR-96-2153, ADA313692.

Knopoff, L., F. Schwab, and E. Kausel, 1973. Interpretation of Lg, *Geophys. J. R. astr. Soc.*, **33**, 389-404.

Li, Y., N.M. Toksoz, and W. Rodi, 1995. Source time functions of nuclear explosions and earthquakes in Central Asia determined using empirical Green's functions, *J. Geophys. Res.*, **100**, 659-674.

Lilwall, R.C., 1988. Regional mb:Ms, Lg/Pg amplitude ratios and Lg spectral ratios as criteria for distinguishing between earthquakes and explosions: a theoretical study, *Geophys. J.*, **93**, 137-147.

Lynnes, C. and R. Baumstark, 1991. Phase and spectral ratio discrimination in North America, *Phillips Laboratory Final Report*, PL-TR-91-2212:1-68, TGAL-91-06.

Matzko, R., 1992. Geology of the Chinese test site near Lopr Nor, Xinjiang Province, China, in *Proc. 14th Annual PL/DARPA Seismic Research Symposium*, pp. 279-303, Phillips Lab, Hanscom, PL-TR-92-2210, ADA256711.

Mueller, C.S., and E. Cranswick, 1985. Source parameters from locally recorded

aftershocks of the 9 January 1982 Miramichi, New Brunswick, earthquake, *Bull. Seism. Soc. Am.*, *75*, 337-360.

Nuttli, O.W., 1980. The excitation and attenuation of seismic crustal phases in Iran, *Bull. Seism. Soc. Am.*, *70*, 469-485.

Nuttli, O.W., 1981. On the attenuation of Lg waves in western and central Asia and their use as a discriminant between earthquakes and explosions, *Bull. Seismo. Soc*, *71*, 249-261.

Nuttli, O.W., 1986a. Yield estimates of Nevada Test Site explosions obtained from seismic Lg waves, *J. Geophys. Res.*, *91*, 2737-2151.

Nuttli, O.W., 1986b. Lg magnitudes of selected East Kazakhstan underground explosions, *Bull. Seism. Soc. Am.*, *76*, 1241-1251.

Nuttli, O.W., 1988. Lg magnitudes and yield estimates for underground Novaya Zemlya nuclear explosions, *Bull. Seism. Soc. Am.*, *78*, 873-884.

Priestly, K.F. and H.J. Patton, 1997. Calibration of $m_b(Pn)$, $m_b(Lg)$ scales and the transportability of the $M_0{:}m_b$ discriminant to new tectonic regions, *Bull Seismol. Soc. Am.*, *87*, 1083-1099.

Quin, H.R. and Thurber, C.H., 1992. Seismic velocity structure and event relocation in Kazakhstan from secondary P phases, *Bull Seismol. Soc. Am.*, *82*, 2494-2510.

Roecker, S.W., T.M. Sabitova, L.P. Vinnik, Y.A. Burmakov, M.I. Golyanov, R. Mamatkanova, and L. Munirova, 1993. Three-dimensional elastic wave structure of the western and central Tien Shan, *J. Geophys. Res.*, *98*, 15,779-15,795.

Sereno, T.J., S.R. Bratt, and T.C. Bache, 1988. Simultaneous inversion of regional wave spectra for attenuation and seismic moment in Scandinavia, *J. Geophys. Res.*, *93*, 2019-2036.

Sereno, T.J. and J. W. Given, 1990. Pn attenuation for a spherically symmetric Earth model, *Geophys. Res. Lett.*, *17*, 1141-1144.

Street, R.L., R.B. Herrmann and O.W. Nuttli, 1975. Spectral characteristics of the Lg wave generated by central United States earthquakes, *Geophys. J. R. Astr. Soc.*, *41*, 51-63.

Tarantola, A., 1987. *Inverse Problem Theory: Methods for Data Fitting and Model Parameter Estimation*, Elsevier, Amsterdam.

Taylor, S.R., Sherman, N.W. & M.D. Denny, 1988. Spectral discrimination between NTS explosions and western U.S. earthquakes, *Bull. Seismo. Soc. Am.* , **78**, 1563-1579.

Vernon, F.V., 1991. Kyrghizstan seismic telemetry network, *IRIS Newsletter, XI*, No. 1, 7-9.

Vergino, E.S. & R.W. Mensing, 1990. Yield estimation using regional $m_{bPn}$. *Bull. Seism. Soc. Am.*, **80**, 656-674.

Xie, J., and B.J. Mitchell, 1990. Attenuation of multiphase surface waves in the Basin and Range Province, part I: Lg and Lg coda, *Geophys. J. Int.*, **102**, 121-137.

Xie, J., 1993. Simultaneous inversion of source spectra and path Q using Lg with applications to three Semipalatinsk explosions, *Bull. Seism. Soc. Am.*, *83*, 1547-1562.

Xie, J., 1996. Synthetic and observational study of Pn excitation and propagation in central Asia, *Phillips Laboratory Scientific Report No. 1*, PL-TR-96-2270, 24 pp, ADA320418.

Xie, J., 1998. Spectral inversion using Lg from earthquakes: Improvement of the method with applications to the 1995, western Texas earth quake sequence, *Bull. Seism. Soc. Am.*, in press.

Xie, J., L. Cong and B.J. Mitchell, 1996. Spectral characteristics of the excitation and propagation of Lg from underground nuclear explosions in Central Asia, *J. Geophys. Res.*, **101**, 5813-5822.

Xie, X-B. & T. Lay, 1994. The excitation of Lg waves by explosions: a finite difference investigation, *Bull. Seismo. Soc. Am.*, **84**, 324-342.

Zhao, X and Ebel, J.E., 1991. Radiation pattern of crustal phases of New England earthquakes, *Gephys. J. Int.*, **106**, 647-655.

Zhu, T.F., K.Y. Chun & G.F. West, 1991. Geometrical spreading and Q of Pn waves: An investigative study in eastern Canada. *Bull. Seism. Soc. Am.*, **81**, 882-896.

THOMAS AHRENS
SEISMOLOGICAL LABORATORY 252-21
CALIFORNIA INST. OF TECHNOLOGY
PASADENA, CA 91125

AIR FORCE RESEARCH LABORATORY
ATTN: VSOE
29 RANDOLPH ROAD
HANSCOM AFB, MA 01731-3010    (2 COPIES)

AIR FORCE RESEARCH LABORATORY
ATTN:  RESEARCH LIBRARY/TL
5 WRIGHT STREET
HANSCOM AFB, MA 01731-3004

AIR FORCE RESEARCH LABORATORY
ATTN:  AFRL/SUL
3550 ABERDEEN AVE SE
KIRTLAND AFB, NM 87117-5776 (2 COPIES)

RALPH ALEWINE
NTPO
1901 N. MOORE STREET, SUITE 609
ARLINGTON, VA 22209

MUAWIA BARAZANGI
INSTOC
3126 SNEE HALL
CORNELL UNIVERSITY
ITHACA, NY 14853

T.G. BARKER
MAXWELL TECHNOLOGIES
8888 BALBOA AVE.
SAN DIEGO, CA 92123-1506

DOUGLAS BAUMGARDT
ENSCO INC.
5400 PORT ROYAL ROAD
SPRINGFIELD, VA 22151

THERON J. BENNETT
MAXWELL TECHNOLOGIES
11800 SUNRISE VALLEY
SUITE 1212
RESTON, VA 22091

WILLIAM BENSON
NAS/COS
ROOM HA372
2001 WISCONSIN AVE. NW
WASHINGTON DC 20007

JONATHAN BERGER
UNIV. OF CALIFORNIA, SAN DIEGO
SCRIPPS INST. OF OCEANOGRAPHY IGPP, 0225
9500 GILMAN DRIVE
LA JOLLA, CA 92093-0225

ROBERT BLANDFORD
AFTAC
1300 N. 17TH STREET
SUITE 1450
ARLINGTON, VA 22209-2308

LESLIE A. CASEY
DEPT. OF ENERGY/NN-20
1000 INDEPENDENCE AVE. SW
WASHINGTON DC 20585-0420

CENTER FOR MONITORING RESEARCH
ATTN: LIBRARIAN
1300 N. 17th STREET, SUITE 1450
ARLINGTON, VA 22209

ANTON DAINTY
HQ DSWA/PMA
6801 TELEGRAPH ROAD
ALEXANDRIA, VA 22310-3398

CATHERINE DE GROOT-HEDLIN
UNIV. OF CALIFORNIA, SAN DIEGO
IGPP
8604 LA JOLLA SHORES DRIVE
SAN DIEGO, CA 92093

DIANE DOSER
DEPT. OF GEOLOGICAL SCIENCES
THE UNIVERSITY OF TEXAS AT EL PASO
EL PASO, TX 79968

DTIC
8725 JOHN J. KINGMAN ROAD
FT BELVOIR, VA 22060-6218 (2 COPIES)

MARK D. FISK
MISSION RESEARCH CORPORATION
735 STATE STREET
P.O. DRAWER 719
SANTA BARBARA, CA 93102-0719

LORI GRANT
MULTIMAX, INC.
311C FOREST AVE. SUITE 3
PACIFIC GROVE, CA 93950

HENRY GRAY
SMU STATISTICS DEPARTMENT
P.O. BOX 750302
DALLAS, TX 75275-0302

I. N. GUPTA
MULTIMAX, INC.
1441 MCCORMICK DRIVE
LARGO, MD 20774

DAVID HARKRIDER
BOSTON COLLEGE
INSTITUTE FOR SPACE RESEARCH
140 COMMONWEALTH AVENUE
CHESTNUT HILL, MA 02167

THOMAS HEARN
NEW MEXICO STATE UNIVERSITY
DEPARTMENT OF PHYSICS
LAS CRUCES, NM 88003

MICHAEL HEDLIN
UNIVERSITY OF CALIFORNIA, SAN DIEGO
SCRIPPS INST. OF OCEANOGRAPHY
9500 GILMAN DRIVE
LA JOLLA, CA 92093-0225

DONALD HELMBERGER
CALIFORNIA INST. OF TECHNOLOGY
DIV. OF GEOL. & PLANETARY SCIENCES
SEISMOLOGICAL LABORATORY
PASADENA, CA 91125

EUGENE HERRIN
SOUTHERN METHODIST UNIVERSITY
DEPT. OF GEOLOGICAL SCIENCES
DALLAS, TX 75275-0395

ROBERT HERRMANN
ST. LOUIS UNIVERSITY
DEPT. OF EARTH & ATMOS. SCIENCES
3507 LACLEDE AVENUE
ST. LOUIS, MO 63103

VINDELL HSU
HQ/AFTAC/TTR
1030 S. HIGHWAY A1A
PATRICK AFB, FL 32925-3002

RONG-SONG JIH
HQ DSWA/PMA
6801 TELEGRAPH ROAD
ALEXANDRIA, VA 22310-3398

THOMAS JORDAN
MASS. INST. OF TECHNOLOGY
BLDG 54-918
CAMBRIDGE, MA 02139

LAWRENCE LIVERMORE NAT'L LAB
ATTN: TECHNICAL STAFF (PLS ROUTE)
PO BOX 808, MS L-175
LIVERMORE, CA 94551

LAWRENCE LIVERMORE NAT'L LAB
ATTN: TECHNICAL STAFF (PLS ROUTE)
PO BOX 808, MS L-208
LIVERMORE, CA 94551

LAWRENCE LIVERMORE NAT'L LAB
ATTN: TECHNICAL STAFF (PLS ROUTE)
PO BOX 808, MS L-202
LIVERMORE, CA 94551

LAWRENCE LIVERMORE NAT'L LAB
ATTN: TECHNICAL STAFF (PLS ROUTE)
PO BOX 808, MS L-195
LIVERMORE, CA 94551

LAWRENCE LIVERMORE NAT'L LAB
ATTN: TECHNICAL STAFF (PLS ROUTE)
PO BOX 808, MS L-205
LIVERMORE, CA 94551

LAWRENCE LIVERMORE NAT'L LAB
ATTN: TECHNICAL STAFF (PLS ROUTE)
PO BOX 808, MS L-200
LIVERMORE, CA 94551

LAWRENCE LIVERMORE NAT'L LAB
ATTN: TECHNICAL STAFF (PLS ROUTE)
PO BOX 808, MS L-221
LIVERMORE, CA 94551

THORNE LAY
UNIV. OF CALIFORNIA, SANTA CRUZ
EARTH SCIENCES DEPARTMENT
EARTH & MARINE SCIENCE BUILDING
SANTA CRUZ, CA 95064

ANATOLI L. LEVSHIN
DEPARTMENT OF PHYSICS
UNIVERSITY OF COLORADO
CAMPUS BOX 390
BOULDER, CO 80309-0309

JAMES LEWKOWICZ
WESTON GEOPHYSICAL CORP.
325 WEST MAIN STREET
NORTHBORO, MA 01532

LOS ALAMOS NATIONAL LABORATORY
ATTN: TECHNICAL STAFF (PLS ROUTE)
PO BOX 1663, MS F659
LOS ALAMOS, NM 87545

LOS ALAMOS NATIONAL LABORATORY
ATTN: TECHNICAL STAFF (PLS ROUTE)
PO BOX 1663, MS F665
LOS ALAMOS, NM 87545

LOS ALAMOS NATIONAL LABORATORY
ATTN: TECHNICAL STAFF (PLS ROUTE)
PO BOX 1663, MS C335
LOS ALAMOS, NM 87545

GARY MCCARTOR
SOUTHERN METHODIST UNIVERSITY
DEPARTMENT OF PHYSICS
DALLAS, TX 75275-0395

KEITH MCLAUGHLIN
CENTER FOR MONITORING RESEARCH
SAIC
1300 N. 17TH STREET, SUITE 1450
ARLINGTON, VA 22209

BRIAN MITCHELL
DEPARTMENT OF EARTH & ATMOSPHERIC SCIENCES
ST. LOUIS UNIVERSITY
3507 LACLEDE AVENUE
ST. LOUIS, MO 63103

RICHARD MORROW
USACDA/IVI
320 21ST STREET, N.W.
WASHINGTON DC 20451

JOHN MURPHY
MAXWELL TECHNOLOGIES
11800 SUNRISE VALLEY DRIVE
SUITE 1212
RESTON, VA 22091

JAMES NI
NEW MEXICO STATE UNIVERSITY
DEPARTMENT OF PHYSICS
LAS CRUCES, NM 88003

ROBERT NORTH
CENTER FOR MONITORING RESEARCH
1300 N. 17th STREET, SUITE 1450
ARLINGTON, VA 22209

OFFICE OF THE SECRETARY OF DEFENSE
DDR&E
WASHINGTON DC 20330

JOHN ORCUTT
INST. OF GEOPH. & PLANETARY PHYSICS
UNIV. OF CALIFORNIA, SAN DIEGO
LA JOLLA, CA 92093

PACIFIC NORTHWEST NAT'L LAB
ATTN: TECHNICAL STAFF (PLS ROUTE)
PO BOX 999, MS K6-48
RICHLAND, WA 99352

PACIFIC NORTHWEST NAT'L LAB
ATTN: TECHNICAL STAFF (PLS ROUTE)
PO BOX 999, MS K6-40
RICHLAND, WA 99352

PACIFIC NORTHWEST NAT'L LAB
ATTN: TECHNICAL STAFF (PLS ROUTE)
PO BOX 999, MS K6-84
RICHLAND, WA 99352

PACIFIC NORTHWEST NAT'L LAB
ATTN: TECHNICAL STAFF (PLS ROUTE)
PO BOX 999, MS K5-12
RICHLAND, WA 99352

FRANK PILOTTE
HQ AFTAC/TT
1030 S. HIGHWAY A1A
PATRICK AFB, FL 32925-3002

KEITH PRIESTLEY
DEPARTMENT OF EARTH SCIENCES
UNIVERSITY OF CAMBRIDGE
MADINGLEY RISE, MADINGLEY ROAD
CAMBRIDGE, CB3 OEZ UK

JAY PULLI
BBN SYSTEMS AND TECHNOLOGIES, INC.
1300 NORTH 17TH STREET
ROSSLYN, VA 22209

DELAINE REITER
AFRL/VSOE (SENCOM)
73 STANDISH ROAD
WATERTOWN, MA 02172


MICHAEL RITZWOLLER
DEPARTMENT OF PHYSICS
UNIVERSITY OF COLORADO
CAMPUS BOX 390
BOULDER, CO 80309-0309


CHANDAN SAIKIA
WOOODWARD-CLYDE FED. SERVICES
566 EL DORADO ST., SUITE 100
PASADENA, CA 91101-2560


SANDIA NATIONAL LABORATORY
ATTN: TECHNICAL STAFF (PLS ROUTE)
DEPT. 9311
MS 1159, PO BOX 5800
ALBUQUERQUE, NM 87185-1159


SANDIA NATIONAL LABORATORY
ATTN: TECHNICAL STAFF (PLS ROUTE)
DEPT. 5736
MS 0655, PO BOX 5800
ALBUQUERQUE, NM 87185-0655


AVI SHAPIRA
SEISMOLOGY DIVISION
IPRG
P.O.B. 2286  NOLON 58122 ISRAEL


MATTHEW SIBOL
ENSCO, INC.
445 PINEDA CT.
MELBOURNE, FL 32940


JEFFRY STEVENS
MAXWELL TECHNOLOGIES
8888 BALBOA AVE.
SAN DIEGO, CA 92123-1506


TACTEC
BATTELLE MEMORIAL INSTITUTE
505 KING AVENUE
COLUMBUS, OH 43201 (FINAL REPORT)


LAWRENCE TURNBULL
ACIS
DCI/ACIS
WASHINGTON DC 20505


PAUL RICHARDS
COLUMBIA UNIVERSITY
LAMONT-DOHERTY EARTH OBSERV.
PALISADES, NY 10964


DAVID RUSSELL
HQ AFTAC/TTR
1030 SOUTH HIGHWAY A1A
PATRICK AFB, FL 32925-3002


SANDIA  NATIONAL LABORATORY
ATTN: TECHNICAL STAFF (PLS ROUTE)
DEPT. 5704
MS 0979, PO BOX 5800
ALBUQUERQUE, NM 87185-0979


SANDIA NATIONAL LABORATORY
ATTN: TECHNICAL STAFF (PLS ROUTE)
DEPT. 5704
MS 0655, PO BOX 5800
ALBUQUERQUE, NM 87185-0655


THOMAS SERENO JR.
SAIC
10260 CAMPUS POINT DRIVE
SAN DIEGO, CA 92121


ROBERT SHUMWAY
410 MRAK HALL
DIVISION OF STATISTICS
UNIVERSITY OF CALIFORNIA
DAVIS, CA 95616-8671


DAVID SIMPSON
IRIS
1200 NEW YORK AVE., NW
SUITE 800
WASHINGTON DC 20005


BRIAN SULLIVAN
BOSTON COLLEGE
INSITUTE FOR SPACE RESEARCH
140 COMMONWEALTH AVENUE
CHESTNUT HILL, MA 02167


NAFI TOKSOZ
EARTH RESOURCES LABORATORY
M.I.T.
42 CARLTON STREET, E34-440
CAMBRIDGE, MA 02142


GREG VAN DER VINK
IRIS
1200 NEW YORK AVE., NW
SUITE 800
WASHINGTON DC 20005

FRANK VERNON
UNIV. OF CALIFORNIA, SAN DIEGO
SCRIPPS INST. OF OCEANOGRAPHY
9500 GILMAN DRIVE
LA JOLLA, CA 92093-0225

JILL WARREN
LOS ALAMOS NATIONAL LABORATORY
GROUP NIS-8
P.O. BOX 1663
LOS ALAMOS, NM 87545        (5 COPIES)

RU SHAN WU
UNIV. OF CALIFORNIA, SANTA CRUZ
EARTH SCIENCES DEPT.
1156 HIGH STREET
SANTA CRUZ, CA 95064

JAMES E. ZOLLWEG
BOISE STATE UNIVERSITY
GEOSCIENCES DEPT.
1910 UNIVERSITY DRIVE
BOISE, ID 83725

TERRY WALLACE
UNIVERSITY OF ARIZONA
DEPARTMENT OF GEOSCIENCES
BUILDING #77
TUCSON, AZ 85721

DANIEL WEILL
NSF
EAR-785
4201 WILSON BLVD., ROOM 785
ARLINGTON, VA 22230

JIAKANG XIE
COLUMBIA UNIVERSITY
LAMONT DOHERTY EARTH OBSERV.
ROUTE 9W
PALISADES, NY 10964